Research Signpost
37/661 (2), Fort P.O., Trivandrum-695 023, Kerala, India

Plant Cell Compartments - Selected Topics, 2008: 41-104 ISBN: 978-81-308-0104-9
Editor: Benoît Schoefs

3 Chlorophyll fluorescence: A wonderful tool to study plant physiology and plant stress

Karel Roháček[1,2], Julie Soukupová[2,3] and Miloš Barták[4]
[1]Biology Centre, p.r.i., Academy of Sciences of the Czech Republic Institute of Plant Molecular Biology, Branišovská 31, CZ-37005 České Budějovice, Czech Republic; [2]Institute of Physical Biology, University of South Bohemia, Zámek 136, CZ-37333 Nové Hrady, Czech Republic; [3]Institute of Systems Biology and Ecology, p.r.i., Academy of Sciences of the Czech Republic Zámek 136, CZ-37333 Nové Hrady, Czech Republic; [4]Masaryk University Faculty of Science, Department of Plant Physiology and Anatomy, Institute of Experimental Biology, Kotlářská 2, CZ-61137 Brno, Czech Republic

Abstract

Photosynthesis belongs to ones of the oldest photophysical and biochemical processes on Earth. A large progress in the research of photosynthesizing organisms was achieved at the end of 20th century by the introduction of modern optical methods and techniques

Correspondence/Reprint request: Dr. Karel Roháček, Biological Centre, p.r.i., Academy of Sciences of the Czech Republic, Institute of Plant Molecular Biology, Branišovská 31, CZ-37005 České Budějovice, Czech Republic. E-mail: rohacek@umbr.cas.cz

allowing to study photosynthetic processes ranging from the subcellular up to the plant canopy level. Among all, chlorophyll (Chl) fluorescence techniques appeared to be a very powerful tool for the nondestructive studying of photochemical and nonphotochemical processes within thylakoid membranes, chloroplasts, plant tissues, and whole plants. In order to use this excellent tool properly, a good understanding of basic principles, procedures, advantages and disadvantages of the fluorimetric[1] methods is necessary. Many excellent books and reviews have been written on these topics, among them the recent book by Papageorgiou and Govindjee, as editors [1] should be emphasized. From this point of view, the present review is written as a practical manual (or a guidebook) for those, who are interested in Chl a fluorescence techniques and their use in the research of primary photosynthesis. This contribution brings to the reader an overview of fundamental principles, basics of instrumental set-ups, experimental protocols, and data analysis related to Chl a fluorescence techniques currently used in photosynthesis research. Herein, an insight in the basic theoretical principles of Chl fluorescence emission, its connection with photochemical and nonphotochemical processes working within thylakoid membranes under light excitation as well as physiological aspects of plant stress are given. With respect to a correct application of the PAM-fluorimetry and Chl fluorescence imaging for plant stress detection and quantification, numerous examples of analysis of Chl fluorescence transients and slow Chl fluorescence induction kinetics are described. A broad attention is paid to the estimation of impact of instrumental properties, external physical, physiological and stress conditions on the Chl fluorescence parameters reflecting actual photosynthetic performance in plants. Some useful methods for a proper data correction are also discussed and demonstrated. The text is supplemented with illustrative figures and references.

Abbreviation list

ABA – abscisic acid; AC – alternating current; APs – pulses of actinic radiation; AR – continuous actinic radiation; Area – parameter derived from fast Chl fluorescence transients; ATP – adenosine-tri-phosphate; B_0^* – non-Q_B-

[1] In contrast to a majority of professional literature, in which the term 'fluorometer' prevails, the terms 'fluorimeter' and 'fluorimetry' are used in this review article. It is due to a grammatical reason applied to the words prefixes and suffixes of the Grecian and/or Latin origins. From this point of view, we can state: fluor-*escent* (a weak glow originating from the mineral fluor-*ite*), *fluori*-meter (an apparatus for recording the fluor-*escence* intensity), *fluoro*-metry (a method determining the amount of the element fluor-*ine* in samples). However, in case of the instruments developed and distributed by authorized world firms (*e.g. PAM-2000* fluorometer, *H. Walz*, Effeltrich, FRG, and others), the frequently-used trade marks of 'fluorometers' are strictly used.

reducing PS II centers; CCD – charge-coupled device; Chl – chlorophyll; DCMU – 3-(3',4'-dichlorophenyl)-1,1-dimethylurea; DAS – dark-adapted state; DP – dark period; Φ_{II} – effective quantum yield of photochemical energy conversion in PS II; Φ_D, Φ_F, Φ_P – quantum yields of nonradiative deexcitation, Chl fluorescence, photochemistry; Φ_{Po} – maximum quantum yield of PS II photochemistry; Φ_{Po}^{ref} – Φ_{Po} of reference sample; F_0, F_0', F_0'', F_0^c – minimum Chl fluorescence yields in dark-adapted state, light-adapted state, dark relaxation phase, after correction; F_M, F_M', F_M'', F_M^c – maximum Chl fluorescence yields in dark-adapted state, light-adapted state, dark relaxation phase, after correction; F_P – maximum Chl fluorescence yield measured when actinic radiation is switched on; F_S – steady-state Chl fluorescence yield in light-adapted state; F_V, F_V', F_V'', F_V^c – maximum variable Chl fluorescence yields in dark-adapted state, light-adapted state, dark relaxation phase, after correction; F(t) – actual Chl fluorescence yield; FD – ferredoxin; FIK – fluorescence induction kinetics; FNR – ferredoxin-$NADP^+$-oxidoreductase; FP – fluorescence parameter; FR – far-red radiation; FY – fluorescence yield; k_D, k_F, k_P, k_Q, k_T – rate constants for heat dissipation, Chl fluorescence, photochemistry, quenching by quencher, excitation energy transfer; λ – wavelength; LAS – light-adapted state; LED – light-emitting diode; LHC – light-harvesting Chl-protein complex; m_A, m_D, m_F – leaf actual mass, dry mass, fresh mass; MR – weak modulated measuring radiation; n_A, n_F – total number of photons absorbed, emitted; NADP – nicotinamide-adenine-dinucleotide-phosphate; NPQ – nonphotochemical Chl fluorescence quenching; NPQ^c – NPQ after correction; NRD – nonradiative dissipation; OEC – oxygen-evolving complex; PAM – pulse amplitude modulation; PAR – photosynthetically active radiation; PFD – photon flux density; PI – photoinhibition; PQ – plastoquinone; PS – photosystem; Q_A, Q_B – primary quinone-type electron acceptors of PS II; q_0 – relative change of F_0; q_E – 'energy-dependent' quenching of Chl fluorescence; q_I – (photo)inhibitory quenching; q_N – (coefficient of) nonphotochemical quenching of F_V; q_N^c – q_N after correction; q_P – (coefficient of) photochemical quenching of F_V; q_T – quenching induced by state 1 - state 2 transition; RC – reaction center; Rubisco – ribulose-1,5-bisphosphate carboxylase/oxygenase; RuBP – ribulose-1,5-bisphosphate; RWC – relative water content; SP – saturation pulse; $\tau_{1/2}$ – half-time of relaxation; t – time; T_S – surface temperature.

1. Introduction

In the last two decades, photosynthetic activities and physiological state of higher plants, lichens, mosses, algae, photosynthetic bacteria, *etc*., are routinely evaluated from the time dependent changes of the chlorophyll (Chl) *a* fluorescence assuming an antiparallel behavior between photochemical processes (*i.e*., charge separation in reaction centers of photosystem (PS) II

followed by an electron transport *via* a set of carriers) and nonphotochemical ones (*i.e*., thermal dissipation and Chl fluorescence). The key photoactive pigment, Chl *a*, is present in all oxygenic photosynthetic organisms and is the almost exclusive photoactive chromophore of all reaction centers (RCs), which convert and store incoming excitation energy in the form of an oxido-reduction potential. Most of the absorbed light energy is utilized in the transport of electrons and protons from water to nicotinamide-adenine-dinucleotide-phosphate ($NADP^+$) and in the phosphorylation of ADP to ATP [1]. Both products are required for incorporation of fixed atmospheric CO_2 into a molecule of sucrose *via* the enzymes of the Calvin-Benson cycle.

Time-course of Chl fluorescence yield (or fluorescence intensity) termed fluorescence induction kinetics (FIK) provides a direct insight into the utilization of the excitation energy by PS II and indirectly also by other complexes within thylakoid membranes [2]. Together with other spectroscopic and biochemical methods, recording of Chl fluorescence helps elucidate many important mechanisms of photosynthesis. At present, Chl fluorescence is widely used as a nondestructive diagnostic tool in photosynthesis research (reviewed in [3-9]). Fluorimeters working on the pulse amplitude modulation (PAM) principle and supplemented with the saturation pulse method [10,11] have allowed to obtain important information on the functioning of the photosynthetic apparatus and photosynthetic activities of plants. They are very helpful in the investigation of acclimatory and adaptive mechanisms activated in plants in order to cope with environmental stresses, such as high light, heat, chilling, dehydration, salinity, malnutrition, *etc*. [12-15].

Contemporary developments in Chl fluorescence imaging enabled to visualize a metabolic status of whole leaves and plants. This technique has been developed in a versatile tool for determining and understanding the heterogeneity in a leaf photochemical efficiency. The application of Chl fluorescence imaging in plant research is growing rapidly, ranging from basic research at the cell and sub-cellular level to biotechnology or remote sensing of plant canopy (reviewed in [16-21]). It is used to visualize photosynthetic heterogeneity caused by not only abiotic and biotic stress factors but also by natural heterogeneity in several physiological processes. It is of high potentials in ecotoxicity testing, monitoring of, *e.g.*, water ecosystems [22], and a high throughput screening for mutants [19]. Furthermore, the potential of Chl fluorescence in remote sensing of vegetation was discussed. Recent imaging instruments are developed to measure the Chl fluorescence dynamics at distances of several meters [21]. The potential for sun-induced Chl fluorescence imaging from outer space by existing imaging spectroradiometers is described by Gower and Borstad [23]. Due to a rapid improvement in the imaging instrumentation and software, it can be expected that the Chl fluorescence imaging will be frequently used not only for the early detection of

plant stress in micro- and macro-scales but also will play an important role in monitoring the ecosystems on a global scale.

In this chapter, we demonstrate that Chl fluorescence can be widely and successfully used as the nonintrusive diagnostic tool in the photosynthesis research. We have focused on many practical aspects of experimental fluorimetric techniques, which allow to study effectively primary photosynthetic processes in higher plants, their organs, tissue, and cell compartments under various physiological and stress conditions. Recently, numerous applications can be found in the field of plant (stress) physiology, algology, agriculture, forestry, horticulture, *etc*. Within the last few decades, due to the better understanding of processes, which affect the Chl fluorescence yield, and also due to a wide availability of commercial fluorimeters, accurate measurements even under field conditions could be performed. Since several factors can lead to a decrease (quenching) of Chl fluorescence, *e.g.*, the excessive irradiance, low/high temperature, drought, toxic chemicals, heavy metals, the interpretation of this fluorescence signal depends on our ability to resolve contributions made by each of these mechanisms. To this purpose, the very useful quantitative information on photosynthetic processes can be decoded from Chl fluorescence kinetic curves using a set of Chl fluorescence parameters. The following text summarizes only the basic parameters derived from the fast (short-term) and slow (long-term) Chl FIKs and is focused on their proper application(s) in photosynthesis research. For more detailed information on theory and practice of Chl *a* fluorescence techniques, we highly recommend the excellent review articles published in [1].

2. Theoretical background

2.1. Thylakoid membrane and linear electron transport

The Chl fluorescence is a physical signal defined as a radiative energy evolved from deexciting Chl *a* molecules (λ = 690 nm for PS II, λ = 740 nm for PS I). Since the arrangement of Chl molecules in pigment-protein complexes of thylakoid membranes may affect a signal in a complex way, a general description of the thylakoid membrane structure and its function is given. For more detailed reading about the organization of thylakoid membranes, numerous books might be recommended (*e.g.*, [24]). Here, only a brief overview with a special respect to those components that may affect Chl fluorescence signals and derived parameters is presented.

The major components of the thylakoid membrane of the chloroplast, important for photosynthetic energy transfer are organized in pigment-protein complexes located in the phospholipidic bilayer of the fluid thylakoid membrane as seen in Fig. 1. Radiation energy capture starts in Chl molecules of light harvesting complexes (LHCs, sometimes referred as PS outer antennae)

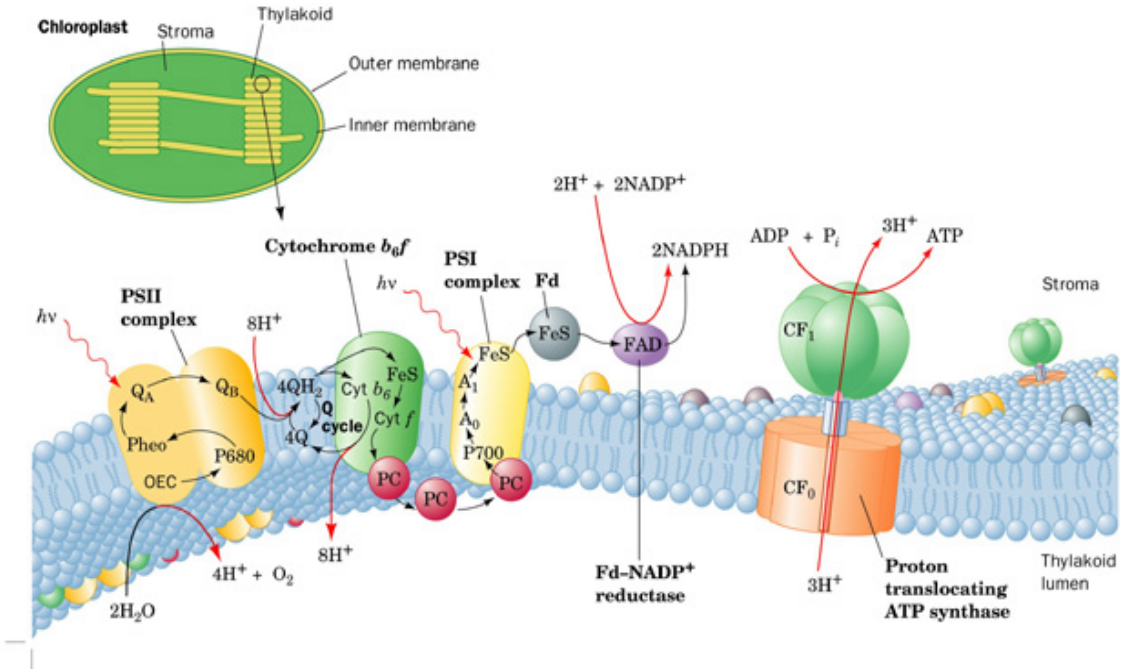

Figure 1. Structure of a thylakoid membrane and its components important for the photochemical electron transport pathway. Key to major abbreviations: OEC – oxygen evolving complex, Pheo – pheophytine, Q_A – quinone A, Q_B – quinone B, QH_2 – hydroxyplastoquinone, FeS – Rieske apparatus, Fd – ferredoxin, PC – plastocyanine, CF_0, CF_1 – coupling factors of ATP synthase (adapted after [24]. Reprinted with the permission of John Wiley & Sons, Inc.).

that are softly attached to core PSs. When phosphorylated, LHCs detached from PS, impairing the transfer of the excitation energy absorbed by LHCs to the reaction center (RC) of PS. LHCs might also aggregate to form groups of three LHCs referred as to LHC trimers [25]. The aggregation may decrease an overall Chl fluorescence signal. In the majority of plants, about tens of LHCs belong to a single PS.

Generally, in LHCs, photons of incident photosynthetically active radiation (PAR) are absorbed. The absorbed energy is transferred to RCs of both PSs in a form of excitons. When absorbed, energy reaches PS II, a transmembrane complex consisting of two major core proteins (D1, D2) and several others (*e.g.*, CP43, CP47 forming the inner antenna). Inside PS II, an intrinsic Chl *a* molecule (an active dimer in the PS II RC) is excited by the absorbed energy and reaches an unstable energetically higher state. The energy of this state is utilized to extract one electron from the RC II special pair of Chl molecules. This electron is transferred to the other PS II core components (Chl *a*, Pheo *a*, and Q_A), and ultimately to Q_B. Q_B^{2-} is a mobile component of the thylakoid membrane. During the electron transfer from an excited Chl molecule to Q_B, the Chl molecule in RC II returns to the ground, electrically

neutral state by receiving an electron from OEC. Then it is awaiting further energy input from LHCs. OEC is softly bound to a tyrozine residue on the D1 protein at a lumenal side of PS II. It acts in the photolysis of water molecules, accompanied with the evolution of oxygen. OEC consists of three proteins of low molecular weight (17, 23, and 33 kDa) [26].

Once when Q_BH_2 has left the Q_B-binding pocket of RC II, a long cascade of consecutive redox-oxidative reactions takes place (Fig. 1). This cascade is known as the photosynthetic linear electron transport chain. It starts from Q_B and follows *via* the plastoquinone pool to a transmembrane protein complex of cytochromes b_6f. In the linear electron transport chain, however, the excitation energy is further transferred to a small (10 kDa) mobile blue-copper protein PC that moves in a lumenal (inner) side of the thylakoid membrane and delivers electrons to PS I. In PS I, the electron is delivered by PC to RC of PS I. Then, with additional energy input from LHCs, the electron is transferred to a phylloquinone (vitamin K) molecule, and over three protein binding Fe-S centers to FD, a partly mobile Fe-S-cluster containing protein located at the stromal side of the thylakoid membrane. The last step of the pathway is catalyzed by FNR, which transfers two electrons to $NADP^+$, yielding NADPH. NADPH is further consumed in the Calvin-Benson cycle. PS I, and FNR in particular, might participate in the linear and cyclic electron transports. The latter starts at FNR from which electrons are transported back to the b_6f cytochrome complex, where plastoquinones are used for the cyclic electron transport.

There are other important components of the thylakoid membrane involved into primary photochemical processes of photosynthesis. Among them, the ATP synthase must be mentioned. ATP synthase is a transmembrane multi-protein structure that utilizes protons coming from OEC. It uses a proton gradient between the lumenal and matrix side as a source of energy to synthesize ATP from ADP and inorganic phosphorus (phosphate group) in a catalytic part of the ATP-complex located in the matrix side of the thylakoid membrane. Last but not least, the thylakoid membrane possesses also some complementary pigments, such as luteins, carotenes, xanthophyll-cycle pigments that serve in a nonphotochemical pathway of dissipation of the over-excitation energy, nonutilized in primary photosynthetic processes. Among them, the role of zeaxanthin, that is converted from vioalxanthin under a stress (see the chapter by Lemoine *et al.*) and a co-occurring high protonation of the lumenal side of the membrane is well known and described elsewhere (*e.g.*, [27-29]). The above mentioned nonphotochemical process quenches effectively Chl fluorescence (see below).

2.2. Chlorophyll *a* fluorescence

After absorption, the excitation energy is transferred to RCs of both PSs, where it drives primary photochemical reactions that initiate the photosynthetic

energy conversion. This photochemical pathway involves the charge separation within PS II RCs followed by the electron transport to $NADP^+$. The electron transport chain is continuously reoxidised by the photosynthetic CO_2 fixation and/or transport of electrons to O_2 (photorespiration, Mehler reaction). The photochemical pathway is not the only way in which the excitation energy is utilized. Thermal dissipation and Chl fluorescence represent other two competitive pathways. The former represents the nonradiative dissipation (NRD) of the excitation energy within PSs to heat. The latter refers to a fluorescence emission caused by the radiative deexcitation of excited Chl molecules (see, *e.g.*, [4,5,30,31]).

The Chl fluorescence originates from deexcitation of the first excited singlet-state of Chl *a* molecules. Chl *b* molecules do not emit fluorescence because excitation energy from Chl *b* is very fast and efficiently transferred to Chl *a* [32]. Under physiological conditions, Chl fluorescence is assumed to be emitted predominantly (about 90 %) from Chl complexes of PS II and represents only about 2-5 % of the absorbed energy [2,3,33]. At room temperature, Chls of PS I complexes are only weakly fluorescent. Moreover, the variable Chl fluorescence belongs strictly to PS II [4]. To quantify the fluorescence from PS II, the quantum yield of Chl fluorescence (Φ_F) is used. It is defined (Eq. 1) as the total number of photons emitted (n_F) divided by the total number of photons absorbed (n_A). Another expression of Φ_F uses rate constants of all competing processes that participate in a return of the excited Chl molecules in PS II to their ground state (*e.g.*, [3-5]).

$$\Phi_F = \frac{n_F}{n_A} = \frac{k_F}{\Sigma k_i} \qquad \text{(Eq. 1)}$$

Here, k_F means the rate constant for Chl fluorescence (a number of fluorescent transitions *per* second) and Σk_i represents the sum of rate constants k_F, k_P (for photochemistry in RC II), k_D (for heat dissipation within LHCs associated with PS II), k_Q (for quenching by quenchers, *e.g.*, carotenoids and/or O_2 triplets), k_T (for energy transfer to nonfluorescent pigments), *etc*. Assuming that k_D includes the rate constants for all nonradiative deexcitation processes (*i.e.*, k_D, k_Q, k_T), the rate constants of three fundamental pathways (k_F, k_P, k_D) are taken into definitions of basic quantities (Eqs. 2-5). They are: the quantum yield of photochemistry (Φ_P), the quantum yield of minimum (Φ_{Fo}) and maximum (Φ_{Fm}) Chl fluorescence, and the quantum yield of nonradiative energy deexcitation to heat (Φ_D) [4,9,34]:

$$\Phi_P = \frac{k_P}{k_P + k_F + k_D} \qquad \text{(Eq. 2)}$$

$$\Phi_{Fo} = \frac{k_F}{k_P + k_F + k_D} \quad \text{(Eq. 3)}$$

$$\Phi_{Fm} = \frac{k_F}{k_F + k_D} \quad \text{(Eq. 4)}$$

$$\Phi_D = \frac{k_D}{k_P + k_F + k_D} \quad \text{(Eq. 5)}$$

In agreement with the energy conservation law, the excitation energy coming into the PS II complexes can not be lost but fully utilized by the photochemical and/or nonphotochemical processes. Thus, the sum of the quantum yields of photochemistry, fluorescence and nonradiative deexcitation equals unity [9] (Eq. 6):

$$\Phi_P + \Phi_F + \Phi_D = 1 \quad \text{(Eq. 6)}$$

Under the assumption, that there are no changes in the absorption cross section of fluorescent Chl species and in the incident light intensity during the recording of fluorescence, the quantum yields Φ_{Fo} (Eq. 3) and Φ_{Fm} (Eq.4) can be replaced by the commonly used relative Chl fluorescence yields (or intensities) F_0 and F_M, respectively (see the definitions below).

2.3. Photochemical and nonphotochemical processes

In healthy plants, up to 80 % of the absorbed energy is transferred under steady-state conditions into the photochemical pathway, only 2 - 5 % represents the Chl fluorescence, and the rest is dissipated to heat [2,35]. Although Chl fluorescence represents a minor competing process of deactivation of excited pigments, the time-varying fluorescence yield (FY) enables to investigate mechanisms by which thylakoids regulate the utilization of the light energy absorbed by PS II complexes. If the efficiency of the photochemical processes increases, it leads to the decrease in quantum yields of the nonphotochemical ones and *vice versa* (see Eq. 6). Thus, the antiparallel relation between the photochemical processes (the charge separation within PS II complexes) and the nonphotochemical ones (heat dissipation, Chl fluorescence) is supposed. Likewise, the increase in dissipation of the excitation energy to heat leads to the quenching of Chl FY below its maximum. If time changes of Chl FY (or Chl intensity) are continuously measured during illumination of a photosynthetically active sample, *i.e.* the so-called Kautsky effect [36,37], the Chl fluorescence induction kinetics (FIK) is

recorded. In photosynthesis research, photosynthetic activities of plants are frequently inferred from the shape (fluorescence transients) of these curves (*e.g.*, [11,30,38-41]).

Co-occurrence of the thermal pathway during Chl fluorescence measurements might bring considerable complications for a correct interpretation of the Chl fluorescence signal. The heat dissipation in chloroplasts can be measured directly by a photoacoustic method (see, *e.g.*, [42-45]). The photoacoustic effect comprises acoustic waves induced by the nonradiative deexcitation of excited states of pigment molecules as a consequence of absorption of the amplitude-modulated light. Main contributors to the acoustic waves in photosynthetic samples are the thermal expansion of cellular organic matter, photosynthetic oxygen evolution, and CO_2 uptake [42,46]. Buschmann [35] has shown that the heat dissipation in PS II was neither low nor parallel to Chl fluorescence. Therefore, it is useful to measure the thermal signal together with Chl fluorescence in order to fully understand the way in which plants convert the absorbed energy.

Capacities of the photochemical and nonphotochemical pathways are usually quantified by the PAM-fluorimetry. Photochemical quenching of variable Chl FY, the coefficient q_P (for definitions see below), is measured on a photosynthetically active, light-adapted sample. For the evaluation of the efficiency of nonphotochemical processes activated during a light phase of photosynthesis (*i.e.*, the build-up of the pH-gradient, state-transitions, ATP-synthesis regulation, inactivation of RCs II, conformational changes within the thylakoid membrane, zeaxanthin formation, *etc*.), the nonphotochemical quenching of variable Chl FY (the coefficient q_N) is applied [5,11,47]. q_N comprises processes predominantly leading to NRD of the excitation energy. The effect of many stress factors on the physiology of plants (*e.g.*, excessive light, low/high temperatures, CO_2 starvation, drought, salinity, heavy metals) results usually in a high reduction of q_P and a pronounced increase in q_N [31,48,49]. Processes that tend to increase q_N are capable to transfer up to 80 % of the absorbed excitation energy to heat. This reversible regulatory and protective mechanism involves conformation changes of thylakoid membranes triggered by the transthylakoidal pH-gradient, state-transitions, and photoinactivation of PS II [50-52]. Some authors have reported [44,53-55] that the energy dependent quenching of variable Chl FY (q_E), the major component of q_N (see below), was connected with the ΔpH- and zeaxanthin-dependent reorganization of the PS II-antenna.

2.4. PAM-principle and saturation pulse method

PAM-fluorimetry is a method based on the principle of the Pulse-Amplitude-Modulation of an induced Chl fluorescence signal. The first

fluorimeter for the detection of modulated Chl fluorescence with a high sensitivity and dynamic capability was developed in the late 80's. It allowed to monitor photochemical processes in PS II and, indirectly, in PS I [10,11,56]. This technique has following main features [9]: (i) the fluorescence inducing radiation ("measuring light") consists of very short (μs-range) repetitively applied pulses of a low and strictly constant intensity; (ii) these pulses do not induce a significant increase of fluorescence yield; (iii) the resulting μs-lasting Chl fluorescence signals coming from photosynthesizing objects are detected by means of a photodiode detector with fast response and large linearity range; (iv) the background signal is rejected using an AC-coupled pulse-preamplifier further processed by a selective-window-amplifier; (v) the switching-on/off artifacts found with conventional lock-in amplifiers are avoided; and (vi) the rapid induction and relaxation Chl fluorescence kinetics can be recorded due to an automatic increase of the measuring light frequency.

A PAM-fluorimeter typically consists of four light sources, which provide quantitatively different radiation inducing changes in a redox state of components of the electron transport chain and causing Chl fluorescence. They are:

(i) the measuring pulsed radiation (MR): MR is provided by a light-emitting diode (LED) as short pulses of a red light with a very low integral photon flux density (PFD < 0.1 μmol m^{-2} s^{-1}). The pulses are 3 μs or 1 μs short, and repeated at the frequencies of 600 Hz or 20 kHz in the *PAM-2000* fluorometer (*H. Walz,* Germany) and 1.6 kHz or 100 kHz in *the PAM101-103* fluorometer (*H. Walz,* Germany) [10,57]. The red radiation having a peak wavelength λ of 650 nm passes through a short-pass filter (λ < 670 nm) and is absorbed by a sample. The emitted Chl fluorescence is detected in a PIN-diode photodetector protected by a long-pass (λ > 700 nm) and heat filters. This very low Chl fluorescence level induced by the measuring beam represents so-called minimum Chl FY, denoted as F_0 (see Fig. 6).

(ii) actinic radiation (AR): The second light source (often an array/panel of varicoloured LEDs or a halogen lamp) generates continuous AR with PFD of up to hundreds of μmol m^{-2} s^{-1}. It triggers the primary photosynthetic processes and, simultaneously, changes in Chl FY. These are detected as the amplitude modulation of a pulsing signal induced by MR.

(iii) saturation pulse radiation (SP): As the source of short SPs (duration of 0.3 to 1.2 s), the halogen lamp is mostly used with white light of very high PFD (up to 10000 μmol m^{-2} s^{-1}). SP temporarily converts all RCs of PS II to the reduced (so-called closed) state. SP also fully reduces all electron carriers in the plastoquinone (PQ) pool. If a flash discharge Xe-lamp is used to generate saturating single (μs-scale) and/or multiple (ms-scale) turnover-flashes, the net accumulation of fluorescence quencher Q_A^- and/or the electron acceptor pool of PS II (PQ pool size) can be measured

as the fast FIK (OJIP transient) [3,58]. During SP, the frequency of MR is automatically increased in order to achieve a better signal-to-noise ratio and time resolution, as well.

(iv) far-red radiation (FR): The source of far-red light (FR) with λ of 735 nm and PFD of approx. 10 μmol m^{-2} s^{-1} is used to promote activity of PS I resulting in a rapid reoxidation of the PQ pool.

Application of the saturating radiation in certain phases of sample illumination by MR and AR is a principle of the saturation pulse method, originally introduced as the "light-doubling" method [38,59]. This method allows to evaluate the photochemical and nonphotochemical quenching in a sample in the following way. At any time of illumination, the fluorescence quenchers Q_A can be fully reduced by SP, *i.e.* the photochemical quenching is completely suppressed (see Fig. 6). In this state, the photochemical processes in PS II are saturated, the rate constant k_P tends to 0, the photochemical quantum yield (Φ_P) becomes zero while the remaining quantum yields (Φ_F, Φ_D) reach the maximal values [9], see Eqs. (2-5). In other words, the absorbed light energy is fully converted to Chl fluorescence and heat. Thus, the maximum Chl FY (F_M' or F_M) is reached. Furthermore, it is assumed that the ratio between quantum yields of fluorescence (Φ_F) and nonradiative deexcitation (Φ_D), as well as the actual nonphotochemical quenching (q_N), do not change during short SP [9,10,30].

2.5. Stress

Plants can maintain and preserve all their vital functions under large variations of the environmental conditions. Among them, incident irradiance, ambient temperature, humidity, supply of water, CO_2 and nutrients, are of main importance. Nevertheless, if the changes exceed the limit of tolerance, serious damages in the structure and function of individual plant cells and organs may occur. According to the general stress theory, the consecutively induced status of the plant, termed stress, generates specific responses on a cellular level (involving general signal responses, adaptation syndromes, and defence responses [60]. Stress leads either to an acquirement of new homeostasis or, under strong stress, to a dysfunction leading to necrosis of the affected organ. If the level of the stress is too strong, the acute stress arises resulting in a rapid damage of plant components and a consequent death of the whole plant, if the stress factor activity is not eliminated in time [61].

The term stress is usually defined as the state of a plant under the condition of a force applied by the stress factor(s) [62,63]. Because the stress is defined solely in terms of plant responses, it is sometimes called a strain and defined as the response to the stress factor and to the force applied to the plant [61]. Two major types of the plant stress are recognized, called abiotic and

biotic stress. The abiotic stress is caused by physical and chemical factors, such as high irradiance, high and low temperatures, water shortage, nutrient deficiency, and also anthropogenic factors, such as pesticides, air pollutants, ozone and photochemical smog, formation of highly reactive species, acid rains, heavy metal load, global climate change, *etc*. The biotic stress includes the defoliation by herbivores, the proliferation of pathogens (viruses, microbes) and fungi, such as mycorrhizes (see the chapters by Fester and, Dumas-Gaudot *et al.*). Environmental conditions that are stressful for one plant may not be stressful for another. If plant tolerance increases as a result of exposure to a prior stress, the plant tends to be acclimated to the stress factor.

The problem of plant stress is more complicated than that of animals and humans, because plants are fixed organisms, *i.e.* they cannot run away the threatening stress factors. Therefore, to cope with the stress factor(s) they have evolved special mechanisms. Plants can develop various protective anatomic structures, such as, *e.g.*, thick cuticle on leaves, inner water reservoirs to avoid water stress. The mechanism of active plant response (stress tolerance) starts when the stress factor acts to the plasma membrane or to the symplast. Then, multiple plant stress responses get started.

The plant stress response can be divided into four phases [61]: (i) response phase - alarm reaction in the beginning of stress, (ii) restitution phase - stage of resistance during continuing stress, (iii) end phase - stage of exhaustion in long-term stress, and (iv) regeneration phase - partial or full regeneration of the physiological function, when the stress factor is removed and the damage was not too intense. At the beginning of the stress, the plant responds by a decline of one or several physiological functions, such as the photosynthetic performance, transport of metabolites, uptake and translocations of ions [61]. Consequently, the plant vitality declines. In the alarm phase, most plants activate the defence mechanism(s) and establish a new physiological standard. In those plants that have no or low stress tolerance mechanisms, acute damage and senescence occur. The long-term stress and/or stress dose overloading the plant defence mechanisms cause severe damages and finally the cell death (the end phase). Once the stress factors disappeared before the senescence processes become dominant, the plant recovers.

All biotic and abiotic stress factors are external signals that are sensed by plant functional receptors. The signal transduction within a plant cell leads to induced metabolic responses (*e.g.*, readjustment of metabolic fluxes), activation of gene expression, enzyme formation, synthesis of stress proteins, stress metabolites, and stress hormones during the first response phase. During the second phase, the plant metabolism is further modified. There are fluent transients and feedback controls between the gene expression and metabolic responses during the restitution phase of the plant stress response. A multitude of stress factors with different modes of action often induce, besides very

specific effects, the same or at least very similar global responses in the plant. For example, both abscisic acid (ABA) and ethylene are involved in a plant acclimation to the water stress, chilling and heat stress, and to oxygen deficiency. Some changes in the gene expression and synthesis of stress-related proteins are induced by different factors, such as the heat shock, salinity, water deficit, and exposure of plants to ABA [62]. Usually, many stress factors co-act simultaneously on a single plant, such as heat, water and high-light stresses during dry, sunny and warm summer periods. Plants often display cross-resistance, or resistance to one stress induced by acclimation to another. This behaviour implies that mechanisms of resistance to several stresses share many common features.

As already mentioned, photosynthetic performance declines at the beginning phase of stress. Furthermore, plant stress considerably changes the chemical and pigment composition of plant leaves, and thus modifies in multiple ways the flow of photons through the leaf [64]. Consequently, the absorption, reflectance, and transmittance properties of leaves are changed in various ways. Stress also changes the relative proportions of absorbed light energy, which are used for photosynthesis and Chl fluorescence induction. Thanks to close relation between changes in Chl FY and photochemical efficiency, Chl fluorescence can be used as the noninvasive tool to detect and study the effects of environmental stress factors on plants from the sub-cellular up to plant canopy level (reviewed in [1]). Chl fluorescence imaging, the experimental technique described in the part 4.1. below, reveals the spatial heterogeneity over the leaf surface. Using distinct Chl fluorescence signatures, Chl fluorescence imaging can be used for an early detection of stress, ***i.e.*** before a visual damage appears, as well as for the tracking the plant defense reactions [19].

3. Integrative chlorophyll fluorimetry

As ‘integrative fluorimetry’, the instrumental techniques and methodologies are understood, which deal with analysis of the Chl fluorescence signal collected/integrated from a rather large area (of tens mm^2) of photosynthetically active samples irradiated by the actinic light sources. These techniques were developed and introduced in photosynthesis research in the late 80’s (see [10,11]). Recently, it is also possible to record the Chl fluorescence signal on a level of single cells using the technique called Chl fluorescence kinetic microscopy (see the part 4.1.).

The instruments capable for this type of measurements can basically cover two measuring approaches: (i) the fast Chl FIK (fluorescence rise) in a very short time interval of *ca*. 0-3 s starting from the dark-adapted, ***i.e.*** photochemically inactive state, and (ii) the slow Chl FIK lasting after some

minutes, during which the fully photosynthetically active state is achieved. Commercially available instruments can use both the relative Chl fluorescence quantum yield, *e.g.*, PAM-fluorimeters-*Walz*, Germany or OS1-FL-*OptiScience*, USA, and the variable Chl fluorescence intensity, *e.g.*, Plant Efficiency Analyser PEA-*Hansatech*, England or Double-Modulation Fluorometer-*Photon Systems Instruments*, Czech Republic (reviewed in [7,9,40,41]). For slow Chl FIK measurements, the PAM-fluorimeters prevail. In the following text, basic methodological principles and some instructive experimental results in both fields of Chl fluorescence measurements are shown and discussed.

3.1. Fast chlorophyll fluorescence induction kinetics

Fast Chl FIK (fluorescence rise) is defined as a Chl fluorescence transient recorded on a dark-adapted plant or photosynthesizing organism during the first few seconds after the sample was exposed to the very short (1-2 s) actinic radiation. The transient has a typical polyphasic shape exhibiting several remarkable Chl fluorescence levels abbreviated as O, J, I, P. Therefore, the kinetics is sometimes reported as the OJIP curve (reviewed in [40]). The O level denotes 'origin' and corresponds to the background Chl fluorescence level, abbreviated also as F_0 in many Chl fluorescence studies. The J and I levels reflect a short-term equilibrium between excitation energy input into PS II and energy outflow due to the redox state of quinones and consequent acceptors of electrons coming from PS II. Typically, the J and I levels are found at 2 and 30 ms [65] after the beginning of exposition to light, respectively. The P ('peak') level represents the maximum Chl fluorescence level reached for the actual excitation radiation. In general, the rise of Chl fluorescence from O to P level reflects gradual accumulation of the reduced quinone Q_A [101]. When the excitation terminates, a gradual, typically exponential, polyphasic decrease of the Chl fluorescence signal is seen. It reflects the dark reoxidation of Q_A and the activity of the other quenchers. After several tens of seconds, the Chl fluorescence decreases to the initial level O (see Fig. 2 and Fig. 3).

Under specific conditions, such as, *e.g.*, high temperature or drought stress, another Chl fluorescence level might appear at the very beginning of Chl fluorescence rise (typically at 300 μs [66]). This level, denoted as K, reflects the heat-induced decrease in the rate of electron transfer from OEC to the tyrosine residue at the donor site of PS II. Recently, a newly classified Chl fluorescence level, denoted as L, was found between O and K, which marks the inflection point that is attributed to connectivity [40]. The presence of typical Chl fluorescence levels might be also altered by a sample used for measurements. While the O, J, I, P levels are apparent in leaves of higher plants,

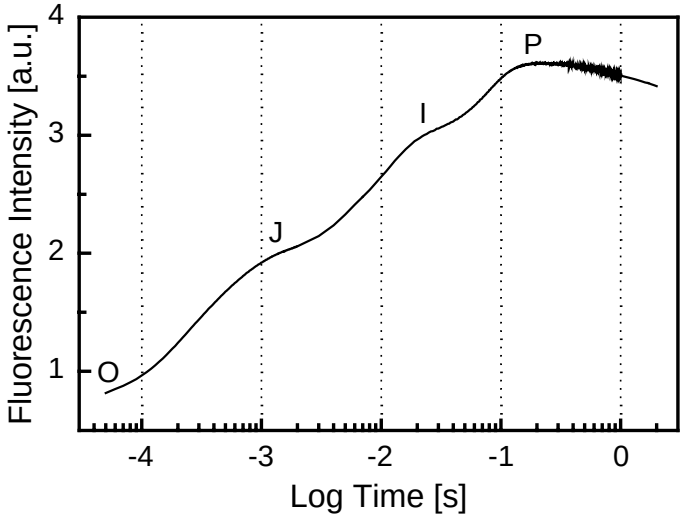

Figure 2. Fast Chl FIK (the Chl fluorescence rise or the OJIP-curve) measured on the primary leaf from 9-day-old wheat (*Tritium aestivum*) seedling by means of Plant Efficiency Analyser (*PEA*, *Hansatech*, Norfolk, UK). The photon flux density of exciting radiation was about 3000 μmol m^{-2} s^{-1} (λ 650 nm). Data courtesy by P. Ilík, Palacký University, Olomouc, Czech Republic.

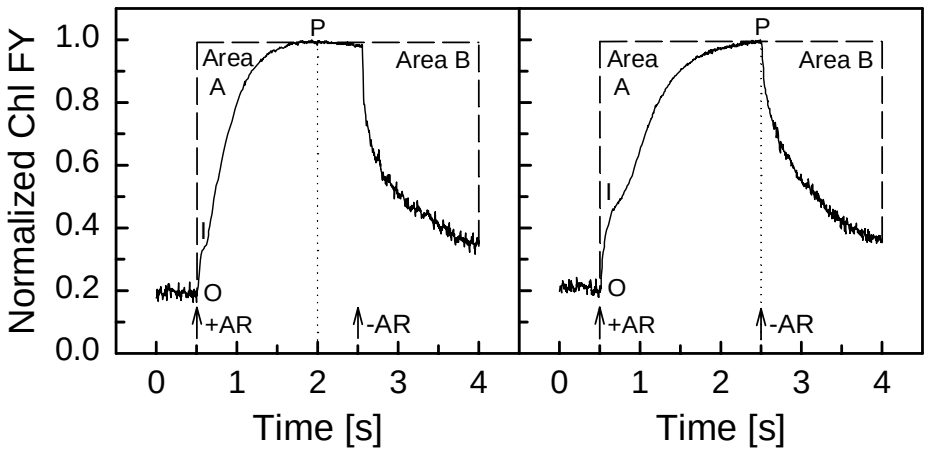

Figure 3. Fast Chl FIKs recorded on leaves of *Lolium perenne* at 20 °C (left graph) and at 5 °C (right graph) after a 40 min gradual lowering of air temperature in a dark. The short-term effect of the temperature drop is apparent as a relative increase in the O and I fluorescence levels and as a prolongation of the time at which P is reached (from 2.0 to 2.5 s). Areas A and B over the rising (actinic radiation switched on, +AR) and decreasing (actinic radiation switched off, –AR) parts of induction kinetics (indicated with arrows) are also altered. The curves were measured using a *PAM-2000* fluorometer (*H. Walz*, Germany) and their graphs are normalized to the individual P levels (0.70 V and 0.81 V for the left and right graphs, respectively). Experimental and plant cultivation conditions are given in [73]. Adapted from [73] with permission of University of Antwerp Press.

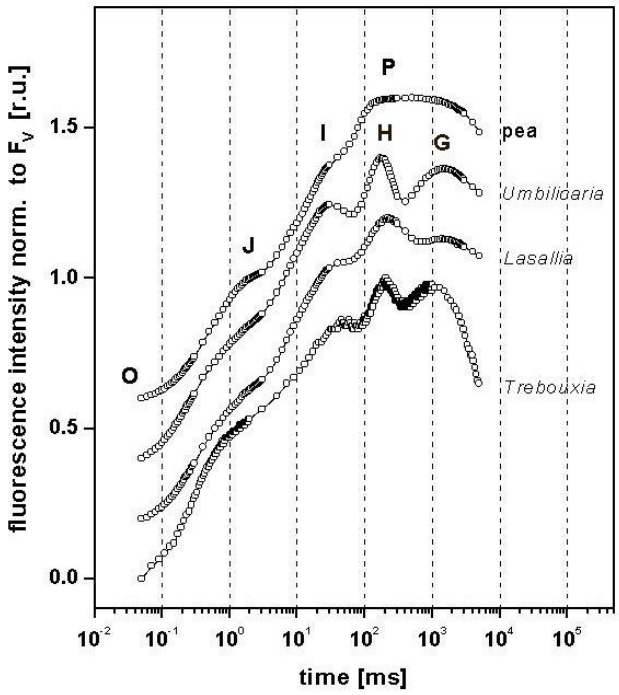

Figure 4. The fast Chl FIKs recorded on pea (*Pisum sativum*) leaves, thalli of two lichen species *Lasallia pustulata* and *Umbilicaria hirsuta*, and lichen symbiotic alga *Trebouxia* sp. Data are normalized to the F_V values. The P level is best seen in the curve obtained with pea, while in symbiotic alga and lichens, the P transition is splitted in two phases, denoted as H and G. These phases are separated by a dip. Reprinted from [77]. Copyright (2006), with permission from Elsevier.

in lower plants, algae and cyanobacteria, no J level is seen when measurements are carried out on isolated PS II membranes [67]. In some species, such as lichens, or symbionts of foraminifers, the P level might exhibit two separate peaks denoted as H and G (*cf.* Fig. 4) – for the nomenclature of the levels see [40,68], for the fluorescence rise analysis see [7].

3.1.1. Basic fluorescence parameters

From fast Chl FIKs, several parameters useful for plant physiological studies can be defined. They comprise: (i) the absolute Chl fluorescence levels and the time, at which they are reached (after the exciting radiation is switched on); (ii) the ratios between distinct Chl fluorescence levels; (iii) the rates of increase/decrease of the Chl fluorescence curve at certain time intervals during induction; and (iv) the areas over increasing/decreasing parts of the Chl FIK. All the parameters (Table 1) can be used to characterize the early processes of energy flow through PS II and they are of a clear biophysical and physiological meaning. Typically, the parameters are used in the assessment of PS II response to a stress or for a detailed study of interrelation between particular

Table 1. The basic Chl fluorescence parameters (absolute Chl fluorescence levels and derived ratios) relevant to the fast Chl fluorescence induction kinetics (compiled after [40,57]).

Parameter	Explanation
F_0	basic (background) Chl FY at the O level (typically at 50 μs)
F_J	Chl FY at the J level (typically at 2 ms)
F_I	Chl FY at the I level (typically at 300 ms)
F_P	Chl FY at the P level (peak); if a saturating excitation light is used, then the maximum Chl FY level (F_M) is reached
F_V	variable Chl FY; $F_V = F_P - F_0$ (or $F_V = F_M - F_0$ as the maximum)
$t_{1/2}$	time at which a half of F_P (or F_M) is reached
t_P	time at which F_P (or F_M) is reached
F_0/F_P	ratio of background to peak Chl fluorescence levels
F_V/F_P	ratio of variable to peak Chl fluorescence levels; if saturating radiation is used for excitation, then the ratio becomes F_V/F_M
V_J	relative Chl fluorescence at the J level; $V_J = (F_J - F_0)/(F_M - F_0)$
V_I	relative Chl fluorescence at the I level; $V_I = (F_I - F_0)/(F_M - F_0)$
Area	area over the Chl fluorescence transient delimited by a horizontal line at F_P; area might be considered either over rising or declining parts of the curve; normalized area, *e.g.*, Area/$(F_M - F_0)$

photochemical processes in PS II and electron carriers in the thylakoid membrane of chloroplasts (reviewed in [7,40,57]).

In fast Chl FIK, the Chl fluorescence levels of F_J, F_I, and F_P might be reached at species-specific times, therefore differing slightly from those reported in the above list. The times also differ according to the value of exciting radiation. The stronger the excitation radiation, the shorter the times to reach F_J, F_I, and F_P. Therefore, the proper time for the F_J, F_I, and F_P evaluation must be checked during experiments (see Fig. 5 and the text in paragraph 3.1.3.).

There are numerous other Chl fluorescence parameters that can be derived from fast Chl FIK, such as: (i) the specific energy fluxes per RC; (ii) the flux ratios, (iii) the energy fluxes per antenna cross section, and many further parameters (reviewed in [40]). The parameters are used in studies focussed on energy flow through PS II.

Many stress factors, such as, *e.g.*, excessive light and heat, cause a change in the structure and functioning of pigment-protein complexes in chloroplastic thylakoid membranes that may lead to a change in the proportion between Q_A-reducing and non-Q_A-reducing PS II centers. The proportion can be evaluated using fast Chl FIKs and specific fluxes through PS II RCs can be calculated [66]. Fast FIKs allow also to evaluate the fraction of the non-Q_B-reducing PS II centers. This evaluation is based on the comparison of two subsequent fast Chl FIKs, the first one recorded in the dark-adapted state of a sample, the other one

after a very short term interval (typically 500 ms in dark) marked as $O^*J^*I^*P^*$. From the two transients, values of F_V, F_M, F_V^*, and F_M^* are taken and used in the following equation [40] to estimate the fraction of non-Q_B-reducing PS II centers (B_0^*) (Eq. 7):

$$B_0^* = 1 - \frac{F_V^* / F_M^*}{F_V / F_M} \qquad \text{(Eq. 7)}$$

3.1.2. Applications in plant stress physiology

Within the last few decades, fast Chl FIKs and the related parameters have been applied in numerous studies devoted to the quantification of stress responses of various plants and photosynthesizing organisms undergoing extreme environmental conditions. Among them, the majority was focused to the effects of excessive (high) light [69], ozone [70], low/high temperature, water stress [71], salt stress, environmental pollution, herbicides [72], pesticides, secondary plant metabolites, *etc*. In the following parts, some instructive examples of fast Chl FIKs used for stress detection in plants and photosynthesizing organisms are presented.

In many studies, a short- or long-term effect of low temperature has been evaluated. In Fig. 3, the short-term effect of a sudden temperature drop on the shape of fast FIK and selected Chl fluorescence parameters is shown. Responses indicated in Fig. 3 might be attributed to low-temperature induced changes in physicochemical properties of a thylakoid membrane, such as the desaturation of fatty acids, lowered fluidity of the membrane, resulting in an altered PQ migration within the membrane and the reoxidation rate of Q_A.

The fast Chl FIKs might be used not only in an estimation of the stress impact on lower and higher plants, but also on foraminifers [74], zooxanthellae of corals [75], and symbiotic organisms like, *e.g.*, lichens [76]. Here, we summarize a recent study [77] focused on the possible causes of the appearance of the H and G levels in fast FIKs, recorded on two foliose lichen *Lasallia* and *Umbilicaria* species hosting a green unicellular alga *Trebouxia* sp. as photosynthesizing partner (see Fig. 4). Fast Chl FIKs recorded on the two lichens exhibit pronounced H and G phases with an apparent dip in between them. It indicates an effective electron flow from the acceptor side of PS II as early as 0.2 s after illumination of the dark-adapted thalli, which is attributable to the photochemical activity of incorporated algae. The dip between the H and G levels is interpreted as an enhanced acceptor side activity of PS I caused most probably by one of the following mechanisms: (i) light-induction of FNR activity, (ii) increase of the cyclic electron transport around PS I, or (iii) activation of the Mehler reaction [77].

Within the last two decades, modeling of fast Chl FIK meets a great success because it helps to understand and estimate particular processes in the thylakoid membrane affecting the shape of the common Chl fluorescence induction kinetics. This mathematical modeling has a great potential in the indication and evaluation of particular steps in energy and electron transfers through PS II [78]. In the last twenty years numerous studies has been focused on modeling the effect of several stress factors using biochemical-based models of different level of complexity. Some authors [79,80] studied an inhibitory effect of DCMU, a PS II acceptor side blocker, on the shape of fast Chl FIK. Also the effect of other stress factors, such as high temperature [81], high irradiance [82] was studied using an approach of the FIK modeling. Recently, attempts are made to compare existing models, unify their assumptions and point out their possibilities to predict efficiency of particular processes [83].

3.1.3. Limitations of the method

The method of FIK recording is fast, noninvasive, allowing repetitive measurements both in a laboratory and the field. Hundreds of transients can be taken even within a single day, what is the reason for the increasing number of application of this technique in many fields of plant physiology. However, some basic requirements must be fulfilled to use the method properly and avoid misinterpretation of raw data.

The FIK measurements start with the dark-adapted samples, *i.e.* with fully open RCs of PS II. Therefore, the selection of a proper length of the dark adaptation period is of crucial importance. Before the measurements, a short test of the dark adaptation period as recommended in [84] has to be made. In general, it consists of gradual prolongation of the dark period with following F_V/F_M determination. Whenever the F_V/F_M ratio reaches its maximum value, the dark period taken before is sufficiently long.

Before any measurement of fast Chl FIK, a selection of the proper excitation light intensity must be made. Throughout the plant kingdom, there are many peculiarities of a leaf structure and anatomy (*e.g.*, cuticle, trichomes, epidermal waxes, presence of absorbing pigments and secondary compounds in the upper epidermis), that may reduce the effective light intensity coming to a chloroplast. Moreover, the difference in composition of pigments existing among green plants and brown, red algae, and cyanobacteria, which highly influences the optical properties and excitation energy utilization within these organisms, should also be taken into consideration, if fast Chl FIKs are measured and discussed for these types of samples [85].

Consequently, the knowledge of the optical and structural properties, and testing the proper light intensity for each species is a necessity in each physiology study. A general rule is that the P level of Chl FY should be

reached before the end of exposition to exciting AR and then it should stay almost constant until AR is switched off. The above mentioned statement according which the absolute values of Chl fluorescence levels J, I, P as well as the respective time of appearance strongly depend on the PFD is demonstrated in Fig. 5. With an increase in PFD, the particular Chl fluorescence levels are shifted up and reached at shorter times. To find the proper times at which the F_J, F_I, and F_P fluorescence levels are reached, the recorded fast FIK should be differentiated and analyzing its shape, the corresponding times of extremes and inflexion points can be evaluated.

To compare properly the fast Chl FIKs measured from different samples or on a sample exposed to defined levels of controlled stress factors, data normalization is necessary because of the sample geometry and some instrumental effects (see the part 3.2.2.). This is achieved by dividing recorded data by a value reached at the certain time of exposition to AR. Usually, the F_0 level is used for normalization, which results in the value of O points being equal to 1. But any Chl fluorescence level might be used for normalization Chl fluorescence transients. It can be easily done using the OJIP-software (*e.g.*, Biolyzer®, Laboratory of Bioenergetics, Geneve, Switzerland). In some cases,

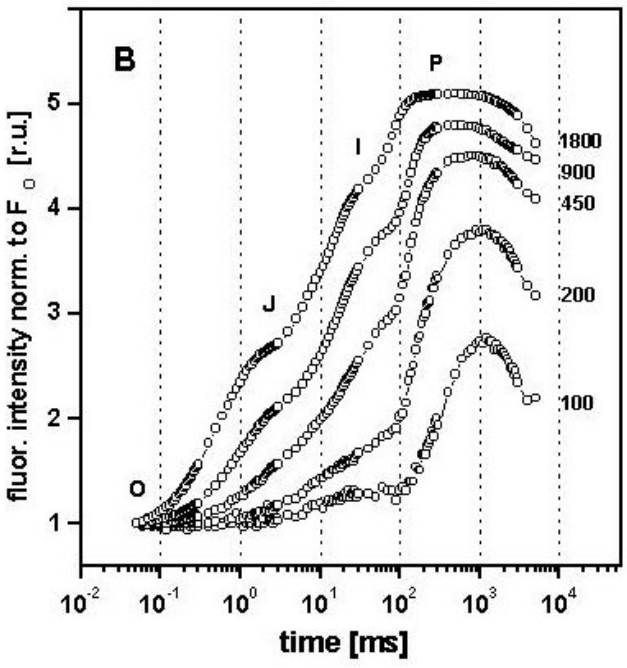

Figure 5. Fast Chl FIKs recorded on a single leaf of pea (*Pisum sativum*) exposed consecutively to increasing excitation photon flux densities (PFD from 100 up to 1800 μmol m^{-2} s^{-1}). The higher the PFD the shorter the time to reach the J, I, P levels. At very low PFDs, some Chl fluorescence levels are missing or not resolved, *e.g.* the J level at 100 and 200 μmol m^{-2} s^{-1}, respectively. Data are normalized to the F_0 level. Reprinted from [77]. Copyright (2006), with permission from Elsevier.

the normalization by division of recorded fast Chl FIKs by the corresponding F_V or F_M values can be recommended [57].

3.2. Slow chlorophyll fluorescence induction kinetics

In the dark-adapted state (DAS), all RCs II of a photosynthetically active sample, generally all PS II RCs, are fully oxidized and components of the nonphotochemical quenching [86,87] are at their minimum. This state (see the part denoted I-DP in Fig. 6) is reached when the whole plant, its leaf or a segment measured is pre-darkened (usually in a special sample holder or chamber) for 10 minutes as minimum. The minimum Chl FY level in DAS (F_0) is recorded when a week modulated MR is applied to the pre-darkened sample. After F_0 is determined, a single short (*ca.* 1 s) light saturation pulse (SP) is triggered causing a transient saturation of photochemical processes in every RC II and an overreduction of the PS II acceptor side, as well. It results in a very fast rise of Chl FY to its maximum level denoted as F_M (see Fig. 6). The correct determination of both reference levels (F_0, F_M) is essential primarily for quantification of nonphotochemical processes activated in the course of a consequent light period, *i.e.* during the actinic radiation (AR).

Typically, pre-darkening of 10 to 20 min is applied (usually 15 min is the optimum). The lower limit of 10 min is due to a back-relaxation of the sample from previous LAS to DAS. The relaxation is of a multi-exponential nature (see III-DARK PERIOD in Fig. 6) [86,90]. Therefore, large alterations in a redox state of the PS II acceptor side can be expected in the first 5 min of the pre-darkening period. In that time, the fast changes in the pH-gradient across the thylakoid membrane play a crucial role, *e.g.* [5,91]. The upper time limit of 20 min might be connected with the in/activation state of enzymes of the carbon reduction cycle, which are light-controlled [92]. Among them, Rubisco, the crucial enzyme of the Calvin-Benson cycle, plays the dominant role. The half-time of Rubisco in/activation *in vivo* amounts to 2-4 min [93]. Moreover, in a dark-light phase, carboxylation of autocatalytically built up RuBP and activation of the RuBP regeneration enzymes are necessary [92]. Therefore, after approx. 30 min in darkness, Rubisco is inactivated and the photosynthetic apparatus tends to diminish all primary photosynthetic processes. When AR is switched on after this too long dark phase, the nonphotochemical processes are largely activated, leading to the dissipation of the excitation energy mostly as heat and to a quenching of Chl fluorescence. It lasts until the carboxylation activity of Rubisco, sucrose synthesis, and supply of inorganic phosphates are restored [93] (*cf.* Fig. 7 and the related text).

During the light period, lasting 5 and more minutes (see part II-LIGHT PERIOD in Fig. 6), the photosynthetic apparatus passes gradually from DAS to the light-adapted state (LAS). In LAS, the electron transport processes and

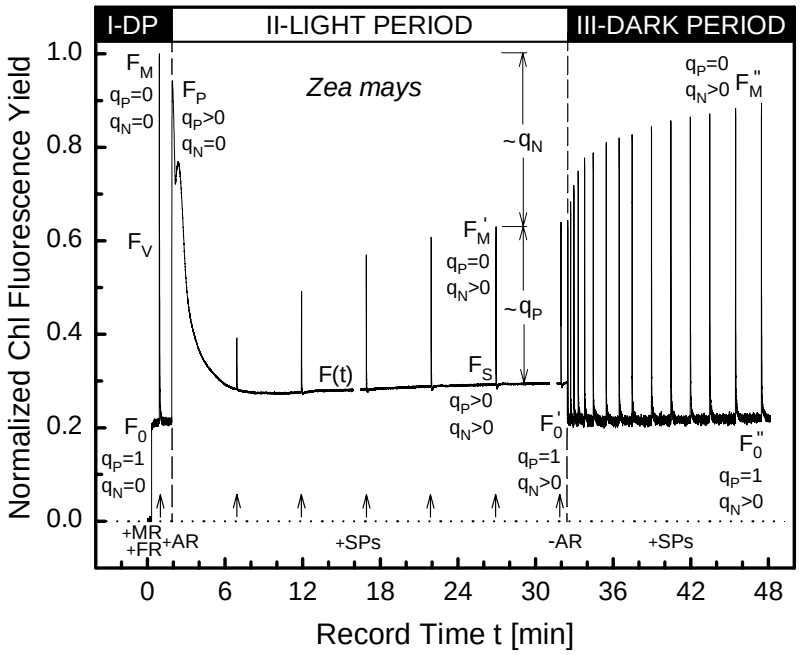

Figure 6. Slow Chl fluorescence induction kinetics recorded *in vivo* by using a portable *PAM-2000* fluorometer (*H. Walz*, FRG) on a fully developed leaf of a potted 10-week-old maize (*Zea mays*). Instrumental settings: measuring radiation (MR) PFD < 0.1 μmol m^{-2} s^{-1} (λ 650 nm), PAM-frequency of 600 Hz, switched on (+MR); actinic radiation (AR) PFD of 180 μmol m^{-2} s^{-1} (λ 655 nm), PAM-frequency of 20 kHz, switched on/off (+AR/–AR); saturation pulse (SP) PFD approx. 3000 μmol m^{-2} s^{-1} (halogen lamp), pulse duration of 0.8 s, PAM-frequency of 20 kHz, set of saturation pulses (+SPs) indicated by arrows (except III-DARK PERIOD); far-red radiation (FR) PFD approx. 10 μmol m^{-2} s^{-1} (λ 735 nm), switched on (+FR). The mean leaf surface temperature during a record was 23.6 ± 0.2 °C, periods of the dark adaptation (15 min, I-DP), light adaptation (30.5 min, II-LIGHT PERIOD), and dark-relaxation (15.5 min, III-DARK PERIOD) were performed in a small ventilated chamber. 1st SP for characterization of the initial DAS was applied in the 14th min of the pre-darkening (I-DP, 1st min of a record), SPs during the light period (II-LIGHT PERIOD) were triggered in 5 min intervals, the dark-relaxation phase (III-DARK PERIOD) was traced by a set of SPs triggered 2, 15, 30, 50, 80, 120, 180, 240, 300, 390, 480, 570, 660, 780, and 900 s after switching AR off. The full record of slow Chl FIK (48 min) consists of three data sets recorded consecutively into a *PAM-2000* memory. Normalization of FIK to F_M was applied. Presumptive values of the photochemical (q_P) and nonphotochemical (q_N) quenching coefficients are highlighted for individual Chl fluorescence levels, *i.e.* F_M, F_0, F_M', F_S, F_0', F_M'', and F_0''.

the coupled biochemical reactions in the carbon reduction cycle equilibrate each other and, consecutively, a steady-state level (F_S) is reached. In the LAS phase, many regulative, light adaptive, and protective mechanisms are activated [5,88]. When SP is applied in the steady-state of photosynthesis, the

maximum Chl FY (F_M') is recorded (Fig. 6). The F_M' level is always below the F_M one because of an overall quenching of Chl fluorescence by processes of the nonphotochemical nature. They include the creation and time changes in the trans-thylakoid pH-gradient, photoinhibitory processes (inactivation and/or photodestruction of PS II RCs), state transitions, zeaxanthin formation trough the xanthophyll cycle activation, conformational changes within thylakoid membranes, *etc.* [4,9,52,55,89]. After switching AR off, the minimum Chl FY in LAS (F_0') is measured after a short pulse (2-3 s) of the weak far-red irradiation (FR) that accelerates the reoxidation of the PSII acceptor side. The switching AR off starts the back-relaxation phase during which the activated (by AR) nonphotochemical processes relax and after a certain time DAS is restored. A transition from LAS to DAS can be monitored as time-dependent changes of minimum (F_0'') and maximum (F_M'') Chl FYs in the so-called dark-relaxation period of the slow Chl FIK (III-DARK PERIOD in Fig. 6).

3.2.1. Basic fluorescence parameters

In general, six primary mutually independent Chl FY levels taken from a record of slow Chl FIK (F_M, F_0, F_P, F_M', F_S, F_0' in Fig. 6) are sufficient for definitions of most Chl fluorescence parameters (FPs), which can be found in literature (see, *e.g.*, [4,8,30,34,35,94]). F_M and F_0 characterize unambiguously DAS, whereas F_M', F_S, and F_0' are specific of LAS. Related Chl FYs are: F_V (maximum variable Chl FY in DAS), F_V' (maximum variable Chl FY in LAS), F_V'' (maximum variable Chl FY in the dark-relaxation phase), F_P (maximum Chl FY measured when AR is switched on), F(t) (actual Chl FY), F_M'' (maximum Chl FY in the dark-relaxation phase), and F_0'' (minimum Chl FY in the dark-relaxation phase). The values of F_V, F_V' and time dependent $F_V''(t)$ are calculated using Eqs. 8-10.

$$F_V = F_M - F_0 \quad \text{(Eq. 8)}$$

$$F_V' = F_M' - F_0' \quad \text{(Eq. 9)}$$

$$F_V''(t) = F_M''(t) - F_0''(t) \quad \text{(Eq. 10)}$$

Here, the most convenient parameters, *i.e.*, those, which are able to give a relevant insight into primary photosynthetic processes in chloroplasts are reviewed (for more details see [34]).

(i) *Maximum quantum yield of PS II photochemistry* [95]

$$\Phi_{Po} = F_V/F_M = 1 - F_0/F_M \quad \text{(Eq. 11)}$$

Φ_{Po} (usually called the F_V/F_M ratio) is the most frequently used parameter, applied often as the indicator of photoinhibition (PI) or other kind of injury

caused to the PS II complexes. It quantifies the maximum photochemical efficiency (capacity) of open RCs II. Φ_{Po} is almost constant for many different plant species when measured under nonstressed conditions and equals to 0.832 [96]. For stressed and/or damaged plants, Φ_{Po} is markedly reduced. Moreover, its value might also be lowered due to fluorescence emission from PS I contributing to the F_0 level [9,97-100].

(ii) *Photochemical quenching of variable Chl fluorescence* [11]

$$q_P = (F_M' - F_S)/(F_M' - F_0') = \Delta F/F_V' \quad \text{(Eq. 12)}$$

Parameter q_P indicates the actual photochemical capacity of PS II in LAS, which is connected with the photochemical energy conversion by charge separation in RCs II. It quantifies the actual fraction of RCs II being in the open state, *i.e.* with reoxidised Q_A [101,102].

(iii) *Nonphotochemical quenching of variable Chl fluorescence* [11]

$$q_N = (F_V - F_V')/F_V = 1 - F_V'/F_V \quad \text{(Eq. 13)}$$

The coefficient q_N reflects the activation of several processes of nonphotochemical nature during the light period and mostly leading to NRD of the excitation energy as heat (thermal dissipation). q_N includes the pH-gradient build up, state-transitions, ATP-synthesis regulation, inactivation of RCs II, conformational changes within thylakoid membranes, activation of the xanthophyll cycle, *etc*. [5,48,52,88,91].

(iv) *Relative change of minimum Chl fluorescence* [103]

$$q_0 = (F_0 - F_0')/F_0 = 1 - F_0'/F_0 \quad \text{(Eq. 14)}$$

q_0 is a coefficient of nonphotochemical nature, directly attributable to the high-energy-state Chl fluorescence quenching. q_0 is connected with the electron flow regulating mechanisms (triggered by the pH-gradient), inactivation of PS II RCs (photoinhibition, photodestruction), xanthophyll deepoxidation, and/or conformation changes within the antenna pigment-protein complexes (state transitions, aggregation of LHC II), *etc*. [64,104-106].

(v) *Nonphotochemical Chl fluorescence quenching* [89]

$$NPQ = (F_M - F_M')/F_M' = F_M/F_M' - 1 \quad \text{(Eq. 15)}$$

The NPQ parameter is often used as an indicator of the excess-radiant energy dissipation to heat in the PS II antenna complexes. The extent of NPQ is linearly correlated to xanthophyll deepoxidation through the xanthophyll cycle. NPQ reflects also the attenuation of the light-harvesting antenna size, PS II inactivation, *etc*. [12,48,107,108].

(vi) *Effective quantum yield of photochemical energy conversion in PS II*; often abridged as 'quantum yield' [109]

$$\Phi_{II} = (F_M' - F_S)/F_M' = \Delta F/F_M' \quad \text{(Eq. 16)}$$

Assessment of Φ_{II} does not require knowledge of the F_0' level, neither does it need previous dark adaptation of the sample. Therefore, it is often used for field investigations. Φ_{II} can be interpreted as the effective quantum yield of the PS II photochemistry related to the actual fraction of photochemically active PS II RCs (q_P). It quantifies the efficiency of the (noncyclic) electron transport, as well as a fraction of photons absorbed in PS II antennae and utilized in the PS II photochemistry. If the photochemical and biochemical processes of photosynthesis are equilibrated under non-stress conditions, Φ_{II} is often correlated with the quantum yield of CO_2 fixation or the rate of photorespiration [9,30,31,57,109].

In the text below, the application of these six principal FPs (Φ_{Po}, q_P, q_N, q_0, Φ_{II}, and NPQ) to the field of plant stress physiology is demonstrated on real examples and concomitant graphs. As it was shown by Roháček [34], the majority of Chl FPs, which are used in the photosynthesis research, might be expressed using the quartet of mutually independent parameters, such as Φ_{Po}, q_P, q_N, q_0.

3.2.2. Main components of the nonphotochemical quenching

This part describes a semi-quantitative method resolving the q_N coefficient into its three main components: (i) the 'energy-dependent' quenching of Chl fluorescence (q_E) related to the pH-gradient build up, (ii) the quenching induced by state 1 – state 2 transitions (q_T) depending on LHC-antenna size regulation, and (iii) the photo-inhibitory quenching (q_I) reflecting photo-inhibition of RC II. These three components of q_N can be distinguished under physiological conditions using analysis of the dark-relaxation phase (III-DARK PERIOD in Fig. 6) of slow Chl FIK [5,86,90]. The q_N relaxation kinetics exhibits an exponential character. It is recorded during transition of the photosynthetic apparatus from LAS back to DAS. The three components differ significantly in their half-times of relaxation ($\tau_{1/2}$) and, thereby, can be mutually resolved [110].

The relaxation of q_N cannot be replaced by relaxation of NPQ because q_N is defined on the basis of F_V and reflects changes in the variable fluorescence (Eq. 13). NPQ, however, covers changes both F_V and F_0 (Eq. 15). If AR is switched off at the steady-state of photosynthesis, the actual value of F_V'' starts to relax in darkness exponentially from the F_V' level to that of F_V (Fig. 6). In principle, estimation of q_E, q_T, and q_I can be made by applying the following three assumptions: (i) the dark relaxation kinetics of q_N and also its

components have an exponential character, (ii) the superposition principle (see Eq. 17) is valid for all components, and (iii) the same reference level (F_V) can be used for definitions of q_N, q_E, q_T, and q_I. The first important fact resulting from these criteria is that q_N is the sum of the three components (see [88,94,111]). Therefore, one can write that

$$q_N = q_E + q_T + q_I \qquad \text{(Eq. 17)}$$

If q_N is determined from given slow Chl FIK, its components can be estimated as described in the following text.

The *energy-dependent quenching of Chl fluorescence* (q_E) reflects the main mechanism involved in the regulation of the excitation energy delivery to match the metabolic demand (reviewed in [112]). This ΔpH-dependent quenching is caused by the intra-thylakoid acidification during light-driven proton (H^+) translocation across the thylakoid membrane coupled with the electron transport pathways. In an excessive light, a lumen pH value below 6 activates the violaxanthin - and other xanthophyll - deepoxidase together with conformational changes in pigment-protein complexes of the PS II antenna. These changes result in thermal dissipation of the excitation energy *via* deepoxidized xanthophyll formation and thus in Chl fluorescence quenching [48,55,88,91]. Ongoing acidification of the lumen may lead to the quenching of up to about 90 % of F_V. This quenching is assumed to be based on the increased rate of the thermal deactivation processes (k_D in Eq. 5) in the PS II complexes [5].

q_E is the quickest relaxing component of q_N, with a half-time of relaxation $\tau_{1/2}^E$ of 30 - 40 s [86, 87]. This implies that the estimation of this component can be expressed by the following equation:

$$q_E \cong 2 \cdot \frac{F_V''(\tau_{1/2}^E) - F_V'}{F_V} \qquad \text{(Eq. 18)}$$

The $F_V''(\tau_{1/2}^E)$-value should be measured at the 30th second of the dark relaxation (see Fig. 6 and Table 2). It is also assumed that the changes in the other two components (q_T, q_I) are negligible during the first 30 s of dark relaxation. The multiplication factor 2 comes from the $\tau_{1/2}$ definition, that is the time in which the exponential function reaches the half value between its maximum and minimum. Eq. 18 gives only a rough estimation of q_E because the kinetic of q_E varies according to the PFD value used as actinic radiation. Furthermore, faster ($\tau_{1/2}^E \leq 10$ s) and much slower ($\tau_{1/2}^E \approx 2$ min) q_E components were also reported [108,113].

If plants are exposed to the excessive radiation (PFD > 1000 $\mu mol \cdot m^{-2} \cdot s^{-1}$) for tens of minutes, photoinhibition of photosynthesis occurs. This phenomenon,

also sometimes called the 'high-light' stress, is often reflected by a pronounced decrease in the F_V/F_M ratio recorded immediately after the photoinhibitory treatment (a 10-15 min pre-dark period is necessary). In some cases, due to strong photoinhibition, full recovery of photosynthesis is not reached even after a long recovery period, which leads to somewhat lowered Φ_{Po} values (Eq. 11) when compared to the pre-photoinhibion state. This *photoinhibitory quenching of Chl fluorescence* (q_I) results from an increase of the nonradiative deexcitation within photosynthetic pigments together with the inactivation and/or photodestruction of D1 proteins in RCs II and the formation of deepoxiated xanthophyll *via* the xanthophyll cycle [48,89]. Long-lasting over-excitation of photosynthetic pigments as well as other kinds of stress factors (drought, low temperatures, heavy metals, CO_2 starvation [97,114-116]) cause a large injury to the photosynthetic apparatus. q_I is the slowest relaxing component of q_N with the half-time of relaxation $\tau_{1/2}^{I}$ of approximately 30 - 40 min [86,87] or even longer [110]. In practice, the dark interval of 15 min (I-DP in Fig. 6) seems to be sufficient for a full relaxation of the q_E component and most of q_T, if present (see below). Thus, the following empirical formulae might enable to estimate q_I from slow FIK recorded in the course or after (photo)inhibitory treatment (Eqs. 19-21):

$$q_I^{DAS} \cong 0.83 - \frac{F_V}{F_M} \qquad \text{(Eq. 19)}$$

$$q_I^{LAS} = q_I \cong \frac{F_V - F_V''(15')}{F_V} \qquad \text{(Eq. 20)}$$

$$q_I^{TOT} \cong q_I^{DAS} + q_I^{LAS} \qquad \text{(Eq. 21)}$$

Here, q_I^{DAS} means a part of the photoinhibitory quenching measured in DAS as the difference between the actual F_V/F_M ratio and the 'optimum' value for Φ_{Po}, *i.e.* 0.83 [96]. The second part, q_I^{LAS}, represents the additional photoinhibitory quenching created during induction phase of Chl FIK by AR. It is calculated using F_V related to DAS and $F_V''(15')$ recorded at the 15th minute of darkness after switching AR off (III-DARK PERIOD in Fig. 6). q_I^{LAS} is identical with the q_I component introduced in Eq. 17. Finally, q_I^{TOT} is the sum of q_I^{DAS} and q_I^{LAS}.

Redistribution of the excitation energy between PS II and PS I can alter depending on external light conditions. In the 'state 1', LHC II is associated primarily with PS II. During the transition to the 'state 2', a mobile part of LHC II becomes functionally uncoupled from the core antenna of PS II due to phosphorylation of the light-harvesting Chl a/b-binding protein (*i.e.*, LHC II-antenna size regulation). Afterward, it migrates from appressed to nonappressed regions of thylakoid membranes. The process of phosphorylation is controlled

via the redox-state of the plastoquinone pool and associated electron carriers [117,118]. It results from the migration that the absorption cross-section of PS II is lowered by detachment of the phosphorylated LHC II and, therefore, the state 1 – state 2 transition results in the increase of the excitation energy transfer to PS I. The observable decrease of Chl FY is expressed as the *state-transition quenching of Chl fluorescence* (q_T) [5].

Adjustment of the energy distribution is particularly important in low, limiting light, when q_T may become the major component of q_N. When a de-phosphorylation of mobile LHCs occurs under the high-light conditions, because of the high trans-thylakoid ΔpH gradient, the contribution of q_T to q_N may be neglected [88]. The half-time of relaxation of this component ($\tau_{1/2}^{T}$) was reported to be approx. 8 min [86, 87]. q_T can be estimated from Eq. 11 supposing the knowledge of the other three remaining components in this way (Eq. 22):

$$q_T \cong q_N - q_E - q_I \qquad \text{(Eq. 22)}$$

Note that q_I in Eq. 22 means the q_I^{LAS} introduced in Eq. 20 due to the q_N definition (Eq. 17).

Under the stress conditions, q_N is markedly underestimated because of a distinct dip in the reference F_M level influencing negatively the F_V value [27]. This problem can be satisfactorily solved using a correction described below (part 3.2.4). Here, as an example, the slow Chl FIK shown in Fig. 6 was analyzed using Eqs. 8-22. Resulted values of above defined FPs are collected in Table 2.

Table 2. Values of the relevant Chl fluorescence levels, six fluorescence parameters (Φ_{Po}, q_P, q_N, q_0, Φ_{II}, NPQ), main components of q_N (q_E, q_T, q_I), and of the total inhibitory quenching (q_I^{TOT}). For calculations, the Chl fluorescence induction kinetics presented in Fig. 6, and Eqs. 8-22 were used.

F_M	F_0	F_V	F_M'	F_0'	F_V'	Φ_{Po}	q_P *)	q_0	Φ_{II} *)	NPQ
1.000	0.213	0.787	0.640	0.217	0.423	0.79	0.82	-0.02	0.54	0.56
F_M''(30")	F_0''(30")	F_V''(30")	F_M''(15')	F_0''(15')	F_V''(15')	q_N	q_E	q_T	q_I	q_I^{TOT}
0.718	0.213	0.505	0.894	0.219	0.675	0.46	0.21	0.11	0.14	0.18

*) $F_S = 0.295$

3.2.3. Applications in plant stress physiology

The most important application of Chl fluorescence techniques in ecophysiological research is the detection and evaluation of stress in plants. PAM-fluorimetry can give excellent insights in the ability of plants to tolerate

environmental stress factors, to cope with a progressive stress and to quantify damages caused by stress factors to the plant photosynthetic apparatus. Various Chl FPs have been used to detect different types of stress, including the light stress, low and high temperature stress, water stress, salt stress, nutrient stress, heavy metals stress, *etc.* (reviewed in [13,64,88,116,119-122]). The above stresses may block or strongly reduce the photosynthetic electron transport whereas increased dissipation of absorbed light energy by heat and Chl fluorescence occurs. The former effect is diagnosed by a decrease in values of the 'photochemical parameters', *e.g.* Φ_{Po}, Φ_{II}, q_P, the latter by an increase in values of the 'nonphotochemical ones', *e.g.* q_N, q_0, NPQ. Here, we report effects only certain types of the environmental stress on primary photosynthesis with an emphasis given on a proper use of the PAM-fluorescence technique and Chl fluorescence parameters.

3.2.3.1. Light-dark cycle

The first example is the measurement of a diurnal course of Chl fluorescence parameters in Norway spruce (*Picea abies* [L.] Karst.). Using this example (see Fig. 7) we demonstrate the principal difference between the day and night physiological regimes of plants [57,123]. Moreover, graphs shown in Fig. 7 point out that the incorrect values of Chl FPs might be rather drawn from records of slow Chl FIK than expected for a fully light adapted steady-state of photosynthesis when too long pre-dark periods (longer than approx. 30 min) are used in PAM-fluorescence experiments. As mentioned above, this effect might be connected with inactivation of Rubisco and, consequently, a stop in the carboxylation process in the Calvin-Benson cycle followed by restrictions in sucrose synthesis. In other words, after about 30 min in dark, the photosynthetic apparatus originally adapted to the 'day regime' (see DAY in Fig. 7) stops primary (light-driven) photosynthetic processes and tends to switch to the 'night regime'(NIGHT in Fig. 7). On the contrary, if the plant is in its night physiology conditions, a short light induction period (*e.g.*, 5 min of AR) used for Chl fluorescence measurements results in a large activation of nonphotochemical processes, which dissipate the excitation energy mainly to heat. This situation lasts until the carboxylation activity of Rubisco, sucrose synthesis, and supply of inorganic phosphates are restored [93], *i.e.* after at least 30 min depending on the light conditions.

From Fig. 7 it follows that the inactivation of the photosynthetic apparatus during the night period leads to an overreduction of the PS II acceptor side during the short-term illumination of spruce needles by AR (170 μmol m^{-2} s^{-1} for 5 min). This situation is accompanied with a pronounced decrease in the efficiency of photochemical processes (see the dip in Φ_{II} and q_P curves) and activation of the nonphotochemical ones (see the increase in NPQ, q_N, q_0 during the dark period) [34]. As expected, no significant changes are observed

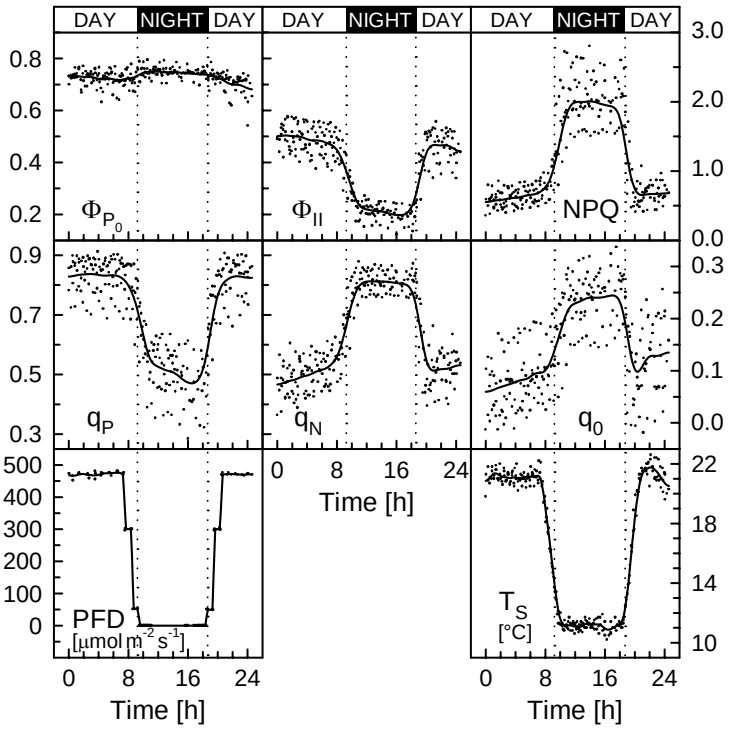

Figure 7. Light/dark cycle of 4-year-old seedlings of Norway spruce (*Picea abies* [L.] Karst.) monitored as the diurnal courses of six Chl fluorescence parameters induced by simultaneous changes of the ambient irradiance (PFD) and temperature of spruce needles (T_S). Each data point corresponds to one Chl FIK recorded *in vivo* using *PAM101-103* fluorometer (*H. Walz*, FRG) under the following conditions: PFD of MR < 0.1 µmol m^{-2} s^{-1} (λ 650 nm, PAM-frequency of 1.6 kHz), PFD of AR 170 µmol m^{-2} s^{-1} (λ 655 nm, PAM-frequency of 100 kHz), switched on for 5 min (F_M', F_S determination) and 5.5 min (F_0' determination), PFD in SP ≈ 9000 µmol m^{-2} s^{-1} (halogen lamp, pulse duration of 0.8 s, PAM-frequency of 100 kHz). Current-year spruce branches of a top whorl with intact needles were fixed in a small chamber and pre-darkened inside for 15 min (F_M, F_0 determination). T_S was measured in the chamber using a Ni/NiCr-thermocouple and PFD in the surroundings of branches using a Lambda-sensor. Experiments started at 11:30 a.m. (time zero) and were repeated on 6 different spruce seedlings. Solid curves in graphs are results of a multiple nonequidistant smoothing from 3 points. For more details see [57].

for the parameter Φ_{Po}. This maximum photochemical efficiency of PS II is the same both in the night and day physiological regimes (if no inhibition processes are activated). A mild decrease of Φ_{Po} at the end of the day-period as well as a small difference between initial Φ_{Po} (t = 0 h) and final Φ_{Po} (t = 24 h) values indicate that external PFD (480 µmol m^{-2} s^{-1} as maximum) and a repetitive closing of spruce branches inside of the sample chamber caused a minor inhibition effect to the photosynthetic apparatus of spruce needles. The mentioned 'chamber effect' and the large photosynthetic variability of

measured plants (reflected in Fig. 7 as the 'broad bands' of experimental data) should also be taken in mind in long-lasting repetitive measurements.

3.2.3.2. Water stress

Because water is an essential substance for plant cells growth and other physiological activities an acute lack in water supply is the most dangerous stress. Water molecules serve as the irreplaceable source of electrons for the linear electron transport chain and protons for the ΔpH-gradient creation across the thylakoid membrane in a light-phase of photosynthesis. In connection with the acute water stress, effects on the photosynthetic efficiency, reduction of electron transport and CO_2 assimilation rates, production of phytohormones (among them ABA plays the most important role), activation of defense and adaptive mechanisms, stomatal regulation, carbon partitioning, modifications in composition of membrane proteins and lipids, *etc.* have been reviewed in [13,14,120,124-126].

Because a water stress causes a gradual loss in the efficiency of photochemical processes in the PS II complexes, its effects can be effectively monitored using the recording of slow Chl FIKs. In higher plants, the PS II functioning is highly resistant to mild water stress. This fact is documented by slow changes in values of Φ_{Po} (Fig. 8). Furthermore, the stomatal closure of C3 plants leaves, growing in water-limited conditions, largely reduces the internal CO_2 concentration in leaves and thus enhances the electron flow with oxygen as the terminal acceptor. Consequently, acidification of the intrathylakoidal space due to the photorespiratory activity of Rubisco and/or the PS I-driven cyclic electron transport results in a photoprotection of the photosynthetic apparatus [13]. All the above mentioned mechanisms lead to a broad activation of nonphotochemical processes under draught stress as reflected by NPQ and other Chl FPs (*e.g.*, [120]).

In Fig. 8, the effect of the acute water stress on photosynthesis in leaf tissue of hibiscus (*Datura arborescens*) plant is demonstrated. To this purpose, three photochemical Chl FPs (Φ_{Po}, Φ_{II}, q_P) calculated from experimental records of slow FIKs (original data not shown), and a relative water content (RWC) were chosen. RWC was determined on a basis of the leaf fresh mass (m_F), dry mass (m_D), and in time of drying actual mass (m_A) as follows (Eq. 23):

$$RWC = 100\ (m_A - m_D)/m_F\ [\%] \qquad \text{(Eq. 23)}$$

For this experiment, a fully developed leaf of an outdoor growing hibiscus plant was used. Once harvested, the leaf was placed in a ventilated pre-dark chamber in a laboratory and kept herein without a water supply. During the period of drying, slow Chl FIKs were recorded using PAM-fluorimeter in given (see Fig. 8) time intervals.

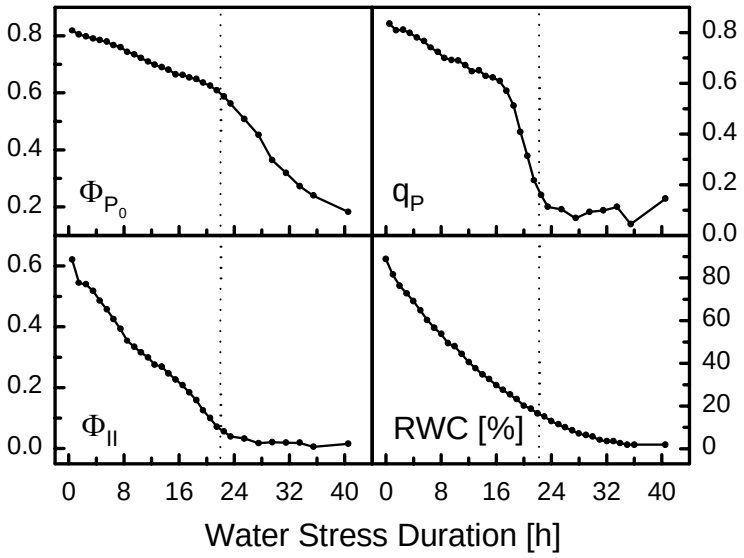

Figure 8. Effect of an increase of water deficiency on the functioning of PS II of a detached leaf of a potted outdoor hibiscus plant (*Datura arborescens*) measured by means of a *PAM-2000* fluorometer (*H. Walz*, FRG). The leaf was kept during the experiment (for 41 h) in dry-air laboratory conditions (late July) inside of a ventilated dark chamber at an unchanged position. The weighting of a leaf together with the removable sample chamber allowed to specify its actual mass and after a final dehydration in a dryer (6 h at 105 °C), the relative water content (RWC) in a leaf tissue was calculated. *PAM-2000* fluorometer settings: PFD of MR < 0.1 μmol m^{-2} s^{-1} (λ 650 nm, PAM-frequency of 600 Hz), PFD of AR 160 μmol m^{-2} s^{-1} (λ 655 nm, PAM-frequency of 20 kHz), PFD in SP ≈ 3000 μmol m^{-2} s^{-1} (halogen lamp, pulse duration of 0.8 s, PAM-frequency of 20 kHz), PFD of FR ≈ 10 μmol m^{-2} s^{-1} (triggered for 3 s). The leaf was kept in a continuous DAS (for the F_M and F_0 recording) interrupted in the given time intervals by a light induction period (5 min of AR for F_M' and F_S determination, 5.5 min to the F_0' determination), (see panel A in Fig. 9). The mean leaf surface temperature was 21.3 ± 0.4 °C while the mean relative humidity in the laboratory was 63 ± 3 %.

Starting from a stage, at which photosynthesis is fully active (stress duration of *ca.* 30 min, *i.e.* starting points in Fig. 8), the data show that drought strongly depresses the utilization of the excitation energy by photochemistry. However, after approx. 22 h of drying (a dotted line in Fig. 8) when the electron transport rate (proportional to Φ_{II}) reaches almost zero and the PS II acceptor side is completely over-reduced (q_P), Φ_{Po} has decreased by only 25 % ($\Phi_{Po} \cong 0.6$). As a consequence, incoming light energy must be dissipated nonphotochemically and high NPQ and q_N values should be seen (data not shown) [120]. Thus, the electron transport rate, proportional to Φ_{II}, and the q_P values decline with the ongoing water stress but faster than Φ_{Po}. Therefore, it is clear that Φ_{Po} (the F_V/F_M ratio) should never be the only Chl FP taken as an indicator of the stress statusimpact to the plant tissue. Therefore, other parameters,

connected with the steady-state photosynthesis, are necessary to describe the status of the photosynthetic apparatus.

The decrease in the efficiency of primary photochemical processes and the increase in thermal dissipation of the excitation energy trapped in PS II units have pleiotropic effects as they will trigger a decline in the activity of some enzymes (sucrose phosphate synthase and nitrate reductase), and an increase in the oxygenic activity of Rubisco as well [13]. These changes are connected with many regulative, conformational and destructive processes of nonphotochemical nature, which occur in the thylakoid membranes during the water stress. They result inevitably in physiological inactivation of a plant tissue. As drought completely inhibits the PS II photochemical capacity [13] (see Φ_{II} and q_P in Fig. 8), the death of plant comes in a final stage of drying.

3.2.4. Limitations of the method

Owing to a fast spreading of fluorescence techniques in fields of plant stress physiology and ecology, it is necessary to warn potential users about particular limitations and bothers of the fluorescence measurements. Correct interpretation of the slow Chl fluorescence kinetic curves and, above all, fluorescence parameters needs a deeper insight in conditions under which they were measured and processed. Among the factors that can influence markedly the results one finds: the duration of the dark adaptation period (see above), the changes in instrumental settings, the changes in sample geometry, the variations of external physical parameters (ambient temperature, irradiance, humidity, CO_2 concentration in a nonventilated laboratory), the fluorescence reabsorption processes, the stress propagation, *etc*. Here, we discuss some of them. For more information (*e.g.*, [1]).

3.2.4.1. Geometry and inhibitory effects

In many experiments, whole plants, their leaves or segments are repeatedly positioned in dark chambers and/or sample holders before measurements using PAM-fluorimetes are performed. During these repetitive measurements of Chl FIKs, the instrumental, the so-called ‘geometry’ effect influences recorded data due to changes in geometry of the sample surface *vs.* fiber-optics of a fluorimeter. It includes nonidentical sample positioning in a sample holder or a measuring chamber, leaf movements and torsions (*e.g.*, during drying), sample/holder thermal dilatations, instabilities of light sources, *etc.* [30,57,127]. Some of these effects can be eliminated in the measuring protocol or corrected during data processing using re-calibration procedures (see below). However, when possible, all instrumental settings and experimental conditions should be kept constant in the given set of measurements.

One of the most serious problems is that values of the majority of Chl FPs depend on a correct determination of the F_M and F_0 reference levels (reviewed

in [34]). If the photosynthetically active system is not in a fully relaxed state, in other words, if the starting, dark-adapted F_M value is depressed for any reason (*e.g.*, due to a strong inhibition of PS II by excessive irradiation, low temperature, draught) then the values of all nonphotochemical parameters are underestimated because F_M represents an input parameter. The reason is that the F_M level in this case does not represent the true maximal value of F_M [12,27]. Regardless, both geometry and inhibitory effects can be satisfactorily corrected, as shown in the following example of the photoinhibition of photosynthesis.

The high-light stress, *i.e.* exposure of plants to irradiance far above the light saturation point of photosynthesis, is one of the most frequently studied stresses (see *e.g.*, [48,88,107,111,115,128]). A decrease in the photosynthetic performance occurs whenever the amount of the absorbed radiation exceeds the potential of electron transport chain and/or linked enzymatic reactions in the Calvin-Benson cycle. This effect, called photoinhibition of photosynthesis, is manifested as the photoinactivation of PS II, degradation of the D1-protein of RC II, destruction of carotenoids, bleaching of chlorophylls, increased lipid peroxidation due to damage by reactive oxygen species, induction of specific early light stress proteins, *etc.* [129,130]. Reduction of PS II efficiency was also correlated with the amount of zeaxanthin in thylakoid membranes, which indicates an involvement of a xanthophyll cycle in the PS II protection against high-light effects and oxidative stress [29,131]. During photoinhibition and immediately after the photoinhibitory treatment, a gradual increase of the heat production was reported [35].

Basically, photoinhibition causes a strong decline in the photosynthetic performance of PS II, which is monitored by depression in its maximum (Φ_{Po}) and actual (Φ_{II}) photochemical efficiency, photochemical capacity (q_P), as well as an activation of the nonphotochemical processes leading to a significant increase of the values of nonphotochemical FPs (*e.g.*, q_N, q_0, NPQ). These facts are demonstrated in Fig. 9 and Table 3, where the results (Roháček, unpublished) reflect the course of photoinhibitory stress in Norway spruce seedlings. Simultaneously, corrections of the instrumental and photoinhibitory effects are elucidated.

In Fig. 9, the first set of 5 FIKs (panel A) represents records of Chl FIKs, which were taken at different time during the PI and recovery experiment. The spruce branches of a top whorl were measured before high-light treatment and then exposed for 30 min to the excessive radiation provided by a sodium lamp (PFD of 3300 ± 100 μmol m^{-2} s^{-1}). Simultaneously, spruce needles were cooled during PI using a fan, and their surface temperature (29 ± 1 ºC) was monitored using Ni/Cr-thermocouple. After PI, the seedlings were kept in a greenhouse under nonphoto-inhibitory cultivation conditions (PFD 300 - 400 μmol m^{-2} s^{-1}/12 h) for recovery. Before the recording of FIKs, the measured branch was fixed in a sample chamber and pre-darkened inside for 15 min prior to F_M and F_0 evaluations.

From the records shown in Fig. 9A follows that PI strongly reduces Φ_{Po} (Table 3). This fact is reflected by a fall in the F_M level and the pronounced increase in F_0. However, if the q_N and NPQ parameters (Eqs. 13, 15) are calculated on the basis of records 'After PI' and 'Recovery (24 h)', then, paradoxically, lower

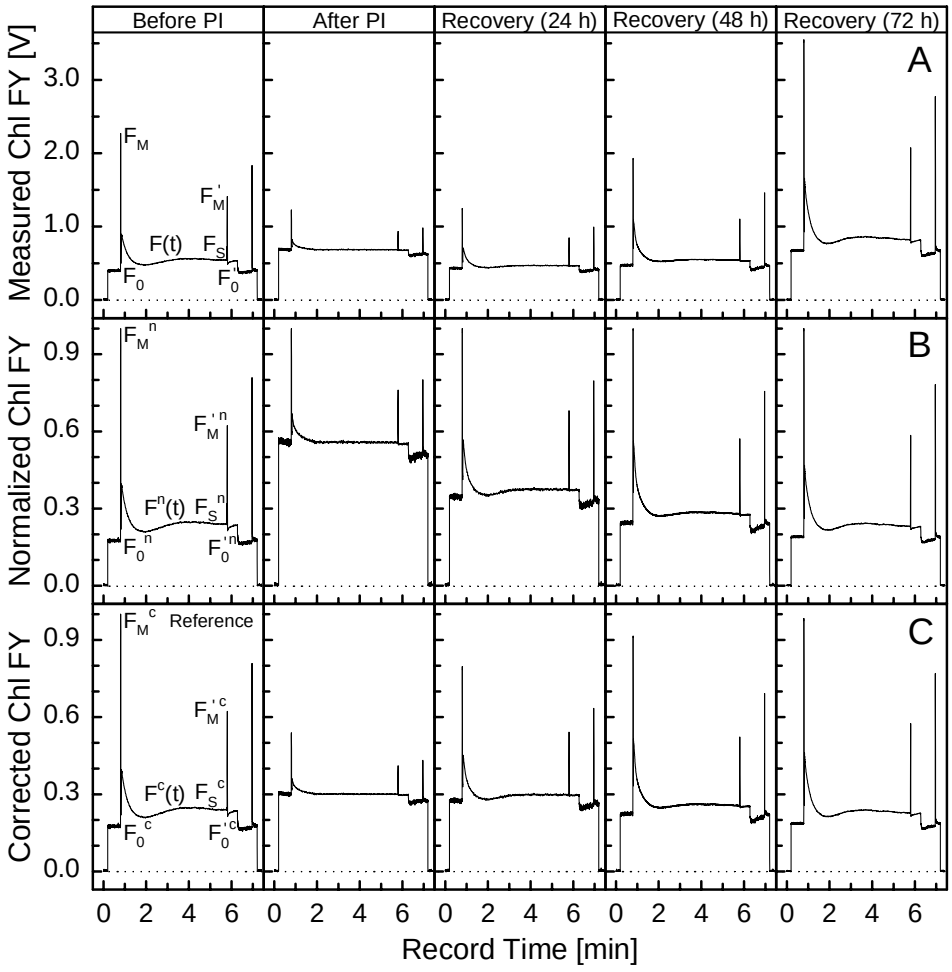

Figure 9. Photoinhibition monitored by sets of slow Chl FIKs recorded *in vivo* on 4-year-old seedlings of Norway spruce (*Picea abies* [L.] Karst.) by means of a *PAM-2000* fluorometer (*H. Walz*, FRG). Each set of 5 FIKs (panels **A** – **C**) represents the Norway spruce status 1 h before photoinhibitory treatment, 20 min after PI by excessive radiation (PFD of 3300 ± 100 μmol m^{-2} s^{-1}), and during 72 h-lasting recovery. The individual data sets differ in a way of data processing (see the text). Instrumental settings: PFD of MR < 0.1 μmol m^{-2} s^{-1} (λ 650 nm, PAM-frequency of 600 Hz), PFD of AR 170 μmol m^{-2} s^{-1} (λ 655 nm, PAM-frequency of 20 kHz), switched on for 5.5 min, PFD in SP ≈ 3000 μmol m^{-2} s^{-1} (halogen lamp, pulse duration of 0.8 s, PAM-frequency of 20 kHz), PFD of FR ≈ 10 μmol m^{-2} s^{-1} (triggered for 3 s). The absolute Y-scale in volts (panel **A**) is a result of signal amplification in the PAM-fluorimeter. Experiments were performed in a greenhouse of the Institute of Plant Molecular Biology (České Budějovice, Czech Republik) in September 1996 by Roháček and Barták (unpublished data).

Table 3. Courses of the photochemical (Φ_{Po}, Φ_{II}) and nonphotochemical (q_N, NPQ) Chl fluorescence parameters during the photoinhibition experiment. For details on corrections of the geometry and photoinhibition effects, see the text.

Parameter	Before PI	After PI	Recovery (24 h)	Recovery (48 h)	Recovery (72 h)
F_M [V]	2.27	1.23	1.25	1.93	3.55[g]
Φ_{Po}	0.824[r]	0.444	0.656	0.754	0.810
Φ_{II}	0.614	0.268	0.451	0.510	0.605
q_N	0.445	0.398[i]	0.439[i]	0.527	0.488
q_N[c]	0.445	0.825	0.645	0.604	0.505
NPQ	0.607	0.315[i]	0.470[i]	0.750	0.709
NPQ[c]	0.607	1.438	0.847	0.912	0.738

[c] corrected value, [g] geometry effect, [i] inhibitory effect, [r] reference value

values of q_N and NPQ after PI are found in comparison with the nonphotoinhibited sample (Table 3). In such a case, values of q_N and NPQ are markedly underestimated because the F_M levels in records after PI do not represent the true maximal F_M values [12]. Another 'strange' result resides in the fact that, after 72 h of recovery from a photoinhibitory treatment in spite of almost full recovery of Φ_{Po} and Φ_{II}, the recorded values of Chl fluorescence signal, F(t), are much higher than those measured for a plant before PI (Fig. 9A and Table 3). From comparison of FIKs obtained before PI, immediately after PI and during the recovery results that both PI and positioning of spruce branches in the sample chamber (geometry effect, *i.e.*, changes in geometry of needles *vs.* fiberoptics, different number of needles measured, *etc.*) significantly affected the recorded Chl fluorescence yields. To correct these effects, additional data processing routines are necessary.

First, the normalization of all FIKs to their individual F_M values should be carried out using the following equation:

$$F^n(t) = \frac{F(t)}{F_M} \qquad \text{(Eq. 24)}$$

In this formula, $F^n(t)$ and F(t) mean the normalized and originally recorded actual Chl FYs, respectively, and F_M is the corresponding maximum taken from the individual record. The normalization (Fig. 9B) eliminates the problem coming from large differences in the absolute Chl fluorescence signal ($F_M^n = 1$ for all normalized FIKs). It also enables to see changes in the F_0, F_S, and F_0' levels in a course of the stress but this procedure does not deal with the paradoxical values found for q_N and NPQ in the previous (nonnormalized) case. Of course, numerical values of individual Chl FPs calculated on a basis of measured (Fig. 9A) and/or

normalized (Fig. 9B) FIKs are identical because FPs are defined as ratios (*e.g.*, [34]), and, therefore, the normalization factor is eliminated.

In the second step, the normalized data should be corrected with respect to some reference parameters which correspond to the stress impact. Based on our experience, we suggest to use the parameter Φ_{Po} as the reference. It is because Φ_{Po} is a very sensitive indicator of any kind of injury caused to the PS II complexes [5,12,88] and reflects immediate changes in the F_M and F_0 levels. The correction formula is (Eq. 25):

$$F^c(t) = F^n(t) \cdot \frac{\Phi_{Po}}{\Phi_{Po}^{ref}} = \frac{F(t)}{F_M} \cdot \frac{\Phi_{Po}}{\Phi_{Po}^{ref}} \qquad \text{(Eq. 25)}$$

The corrected FIK, $F^c(t)$, is obtained by multiplying $F^n(t)$ by the ratio between Φ_{Po} of the sample to be corrected and of the reference sample, Φ_{Po}^{ref}, for instance that obtained with an unstressed sample. Optimally, Φ_{Po}^{ref} can amount to 0.832 [96].

The resulting corrected curves are presented in Fig. 9C. Φ_{Po} and F_M values used for the calculations are displayed in Table 3. The resulting FIKs reflect correctly the expected trends, namely: the highest F_M and the lowest F_0 recorded before PI, a dip in F_M accompanied with a steep rise in F_0 during PI treatment, and the exponential-like relaxation of F_M during the recovery. These findings correspond to the well-known fact that PI causes a breakdown of the D1-protain in PS II and requires a regeneration of several hours in the dark [5,111]. This recovery phase is clearly demonstrated in Fig. 9C. As seen, the capacity for reparation of the damaged components of the photosynthetic apparatus was sufficient to re-establish the fully photosynthetically active state after approx. 72 h of Norway spruce recovery.

Corrected FIKs in Fig. 9C permit to recalculate values of the nonphotochemical parameters q_N and NPQ using the F_M^c and F_0^c levels of the 'reference sample' ($F_M^{c\,ref}$, $F_0^{c\,ref}$). These corrected parameters q_N^c and NPQ^c are deduced from Eqs. 13 and 15:

$$q_N^c = 1 - F_V'^c / F_V^{c\,ref} \qquad \text{(Eq. 26)}$$

where $F_V'^c = F_M'^c - F_0'^c$, $F_V^{c\,ref} = F_M^{c\,ref} - F_0^{c\,ref}$

$$NPQ^c = F_M^{c\,ref} / F_M'^c - 1 \qquad \text{(Eq. 27)}$$

In practice, the variables $F_V'^c$ (for q_N^c) and $F_M'^c$ (for NPQ^c) are taken consecutively from the set of corrected FIKs while the reference values ($F_V^{c\,ref}$ for q_N^c, $F_M^{c\,ref}$ for NPQ^c) stay constant within the calculations. Resulted q_N^c and NPQ^c values are presented in Table 3. As seen, the incorrect q_N and NPQ

values (indicated by the index 'i' in Table 3) are fully eliminated in this way. Thus, using the described procedure, the photoinhibitory effect can be successfully corrected (see also the next text).

3.2.4.2. Correction of the effects of ambient temperature and irradiance

Two other environmental parameters, other than water availability, significantly affect photosynthesis. They are the external photon flux density of the photosynthetically active radiations (PAR) and the ambient temperature. It is well established that the *in vivo* Rubisco activity controlled by Rubisco activase decreases with temperature increase above the optimum [132,133]. Both the high-light over-excitation and heating of the photosynthetic apparatus are harmful for photosystems, especially PS II. Similarly, the PS II photochemical activity, but not light absorption, decreases significantly at low temperatures and, therefore, the sensitivity of the photosynthetic apparatus to photodamage increases [31,48]. To minimize damages to PS II complexes, the xanthophyll cycle-dependent q_N-protective mechanism is activated. It maintains a high proportion of Q_A in the oxidized state whilst low temperatures strongly limit the capacity of photosynthesis [134]. In case of the long-term low-temperature stress, the substantial part of absorbed radiation is dissipated to heat [27].

It is evident that changes in temperature and irradiance influence photosynthesis and Chl fluorescence. For example, using simultaneous measurements of a leaf gas exchange and Chl fluorescence emission, the pronounced effect of temperature on the rate of leaf net photosynthesis and electron transport rate was found (*e.g.*, [135,136]). Values of both parameters decreased significantly with temperature below 15 °C and above 35 °C. Further, the photosynthetic optimum was found around 20 °C. Our own results [123] are in a good agreement with these findings. Both temperature and light stress affect negatively the PS II complexes resulting in changes in the F_M and F_0 levels. As in the previous case of PI, all Chl FPs based on these two reference levels are negatively affected and, thus, should be corrected. In the following text and graphs (Figs. 10 and 11), the correction procedures based on Eqs. 25-27 are explained and applied.

For this correction, results obtained with Norway spruce seedlings exposed to varying ambient temperature and irradiance were utilized. Cultivation conditions and experimental settings were described in [57,123] and also mentioned above in the part 3.2.3.1. In the first case discussed below (see Fig. 10), the values of the five basic Chl FPs (Φ_{Po}, Φ_{II}, q_P, q_0, q_N) were derived from slow Chl FIKs measured on seedlings during a controlled change of ambient temperature from +4 °C to +34 °C. Prior to the experiments, seedlings were cooled during 70 min from the cultivation temperature of +21 °C to the minimum and then slowly heated (by 1 °C *per* 15 min) to the maximum temperature under constant irradiance. In the second case (Fig. 11), the values

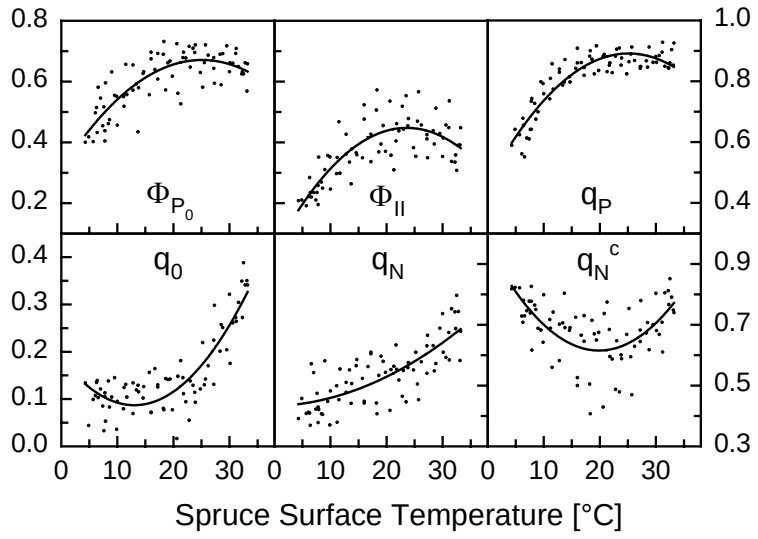

Figure 10. Effect of the rise of the ambient temperature from +4 °C to +34 °C on primary photosynthesis of six 4-year-old seedlings of Norway spruce (*Picea abies* [L.] Karst.) as monitored using selected Chl FPs. Each point in the graphs corresponds to one slow Chl FIK recorded *in vivo* using a *PAM101-103* fluorometer (*H. Walz*, FRG) under the same conditions as described in the legend of Fig. 7. During the measurements, the ambient irradiance was kept at 375 ± 3 μmol m^{-2} s^{-1}. For the parameter q_N^c, the correction of q_N was performed as explained in the text (Φ_{Po}^{ref} = 0.731, *i.e.* the maximum Φ_{Po}-value in a set). Solid curves fitted within experimental data are polynoms of the 2nd order. Data adapted from [123].

of same Chl FPs were derived from slow Chl FIKs measured on spruce seedlings during a change of the ambient irradiance from 3 up to 700 μmol m^{-2} s^{-1} under constant temperature.

As seen from Figs. 10 and 11, the efficiency of photochemical (Φ_{Po}, Φ_{II}, q_P) and nonphotochemical (q_0, q_N) processes in higher plants depends markedly on the ambient temperature and irradiance. For spruce seedlings, the long-term temperature optimum (20 - 25 °C, Fig. 10) as well as the light optimum (300 - 400 μmol m^{-2} s^{-1}, Fig. 11) were found. Below and above these optima, the regulative, defense, and other mechanisms of nonphotochemical nature are activated whereas the photochemistry is reduced. These processes are clearly reflected by corresponding FPs. For example, the temperature decrease below the optimum (+23 °C, Fig. 10) causes pronounced changes in Φ_{Po}, Φ_{II}, q_P and q_N. The photochemical energy conversion in PS II (Φ_{Po}) and the rate of a linear electron transport (Φ_{II}) are strongly reduced by low temperatures [123,136]. In case of PFD (Fig. 11), the pronounced increase in q_N and q_0 is apparent for PFD below 150 μmol m^{-2} s^{-1} and above 600 μmol m^{-2} s^{-1}. The effect of the former PFD might be related to the Calvin-Benson cycle inactivation under the low light (see Fig. 7), the effect of the later PFD reflects

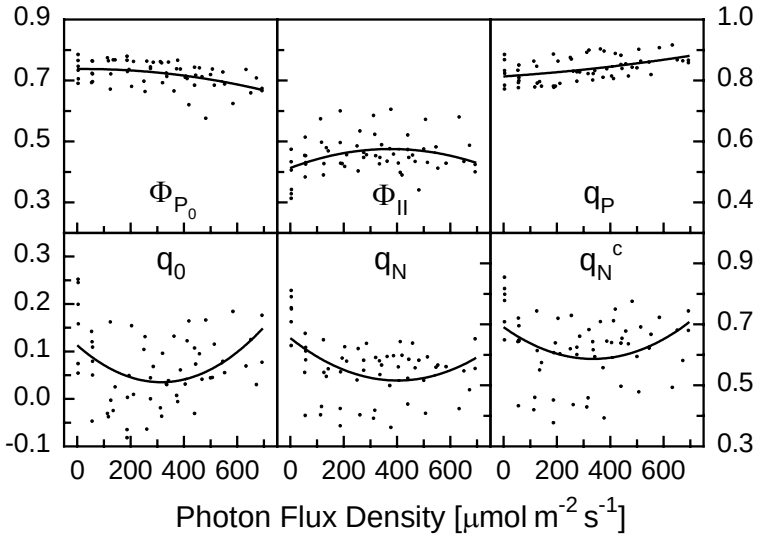

Figure 11. Effect of a change in the ambient irradiance (PFD ranged from 3 to 700 μmol m^{-2} s^{-1}) on the primary photosynthesis of six 4-year-old seedlings of Norway spruce (*Picea abies* [L.] Karst.) as monitored using selected Chl FPs. Each point in graphs corresponds to one slow Chl FIK recorded *in vivo* using a *PAM101-103* fluorometer (*H. Walz*, FRG) under the same conditions as described in the legend of Fig. 7. During the measurements, the ambient temperature was equilibrated to +20.7 ± 0.4 °C. For the parameter q_N^c, the correction of q_N was performed as explained in the text (Φ_{Po}^{ref} = 0.785, *i.e.* the maximum Φ_{Po}-value in a set). Solid curves fitted within experimental data are polynoms of the 2nd order. Data adapted from [123].

activation of photoinhibitory processes leading to the thermal dissipation of the excessive radiation within the thylakoid membranes [29,48].

In contrast to other FPs, q_N showed no temperature optimum (Fig. 10). This finding is connected with the inhibitory effect described above. Due to the strong effect of the ambient temperature on the F_M and F_0 levels demonstrated in Φ_{Po} (Fig. 10), the calculated q_N values are markedly underestimated, especially for low temperatures. To correct this negative effect, the equations 11, 13, 25, and 26 can be used in the following way (Eq. 28):

$$q_N^c = 1 - \frac{F_V'^c}{F_V^{c\,ref}} = 1 - \frac{F_V'/F_M}{F_V^{ref}/F_M^{ref}} \cdot \frac{\Phi_{Po}}{\Phi_{Po}^{ref}} = 1 - \frac{F_V'}{F_M} \cdot \frac{\Phi_{Po}}{(\Phi_{Po}^{ref})^2} = 1 - \frac{F_V'}{F_V} \cdot \frac{F_V}{F_M} \cdot \frac{\Phi_{Po}}{(\Phi_{Po}^{ref})^2}$$

$$q_N^c = 1 - (1 - q_N) \cdot \frac{(\Phi_{Po})^2}{(\Phi_{Po}^{ref})^2} \qquad \text{(Eq. 28)}$$

If q_N values are recalculated using Eq. 28, the corrected parameter q_N^c satisfies the presumed parabolic course with the temperature optimum around +20 °C (see Fig. 10). In case of the q_N dependence on PFD (Fig. 11), the correction of q_N using Eq. 28 has a less pronounced effect because there are only mild

changes in F_M and F_0 found for the low to the optimum irradiance (see the Φ_{Po} tendency in Fig. 11).

In the same way, correction formulae for other nonphotochemical FPs can be derived. For NPQ and q_0 we have (Eqs. 29 and 30):

$$NPQ^c = \frac{F_M^{c\,ref}}{F_M^{'c}} - 1 = (NPQ + 1) \cdot \frac{\Phi_{Po}^{ref}}{\Phi_{Po}} - 1 \qquad \text{(Eq. 29)}$$

$$q_0{}^c = 1 - \frac{F_0^{'c}}{F_0^{c\,ref}} = 1 - (1 - q_0) \cdot \frac{\Phi_{Po}\,(1 - \Phi_{Po})}{\Phi_{Po}^{ref}\,(1 - \Phi_{Po}^{ref})} \qquad \text{(Eq. 30)}$$

Here, NPQ and q_0 denote values of FPs calculated from Chl FIKs recorded in experiments, NPQ^c and $q_0{}^c$ are the corrected ones.

Finally, it should be mentioned that the physical parameters (*i.e.*, the ambient temperature, irradiance, humidity) are mutually dependent. Because they strongly effect photosynthesis, it is of high importance to keep them constant during the measurements. However, it can be hardly fulfilled in the field experiments where the physical parameters vary dynamically over a wide range of values. In such a case, the multi-parametric calibration measurements should be performed. The calibrations are usually difficult and time consuming. Therefore, for the environmental photosynthetic fluorescence measurements, the parameter Φ_{II} (Eq. 16) is widely used. Φ_{II} holds information on the actual overall photochemical energy conversion in PS II and can be measured very fast in LAS because it does not require dark pre-adaptation of the sample, nor a knowledge of the F_0' level [57,109].

4. Chlorophyll fluorescence imaging

4.1. Basic principles

Photosynthesis and consequently Chl fluorescence emission can be altered by various internal factors (differences in physiology during development, pigment composition, senescence, *etc.*) and external ones (abiotic and biotic stress factors) that vary over the surface of leaf or plant. Such heterogeneity has been recently studied by the means of the Chl fluorescence imaging techniques, which are noninvasive and fast in data acquisition and processing.

Imaging of Chl fluorescence allows the examination of thousands of small points (*i.e.*, pixels in the Chl fluorescence image) with fluorescence transients located in discrete areas. These transients can be analyzed individually or grouped into images and assigned to individual objects, such as plants, leaves, leaf segments, cells or cell compartments. Consequently, Chl fluorescence imaging systems can provide detailed information about spatial and kinetic heterogeneity over the surface of a plant leaf or a whole plant. Chl fluorescence

imaging also allows to analyze a large number of small objects simultaneously in one experiment. These possibilities distinguish the imaging systems from the nonimaging integrative fluorimetry.

Probably, the first Chl fluorescence imaging was performed in the 1930s, when Kautsky and Hirsch [36] placed the dark-adapted plant into blue light and observed the Chl fluorescence induction by their eyes. The first imaging instrument was described by Omasa *et al*. [137] and soon thereafter by Daley *et al*. [138]. The imaging system, working on the PAM-principle, was firstly employed in 2000 to image Chl fluorescence distribution both on leaf [139] and cell level [140]. References concerning Chl fluorescence imaging systems before 2005 are available in [141] and [19]. Recently, a system for imaging Chl fluorescence of aquatic phototrophs has been introduced [142].

Oxborough [20] has divided the Chl fluorescence instruments into two groups: (i) high resolution systems, which can resolve features at the cellular and sub-cellular levels (*e.g*., [20,140,144-146]), and (ii) low resolution systems, which can resolve features down to the level of small groups of cells (*e.g*., [138,139,143,147-152].

The instruments designed for Chl fluorescence imaging typically consist of light sources, an imaging detector, a control unit, a power supply, and a computer (Fig. 12). The majority of Chl fluorescence imaging systems is based on cameras that utilize a charge-coupled device (CCD) sensor to image captured Chl fluorescence emission. All Chl fluorescence imaging systems that measure F_M and F_M' use one or more light sources to provide: (i) actinic illumination that drives photochemistry and induces the fluorescence transient, (ii) saturating multiple turnover pulses to measure F_M and F_M', and (iii) measuring flashes to excite background Chl fluorescence during imaging (the measuring protocol is reviewed, *e.g*., in [153]; see above).

The measuring light is usually provided by LEDs, which serve as a versatile light source in Chl fluorescence imaging [139,140]. The duration of flashes from LEDs can be controlled down to the sub-microsecond range, and irradiance levels can be set from low irradiance to light exceeding sunlight [19,154]. Similarly to nonimaging PAM fluorimeters, recent imaging fluorimeters are designed to control the opening time of the CCD camera to be synchronous with the short measuring light [139]. The advantage of application of the PAM method to Chl fluorescence imaging is that it can be used under a wide range of light sources of different spectral characteristics [19,20,139]. Also actinic illumination is usually provided by LEDs. Saturating pulses can be generated either by LEDs or by other light source, *e.g.* a halogen lamp. Detailed information about the light sources, detectors, their properties and use in Chl fluorescence imaging has been recently reviewed [19,20].

The software that drives the instrumentation and analysis is a critical factor in determining the usefulness of the Chl imaging fluorimeter [19]. It controls the

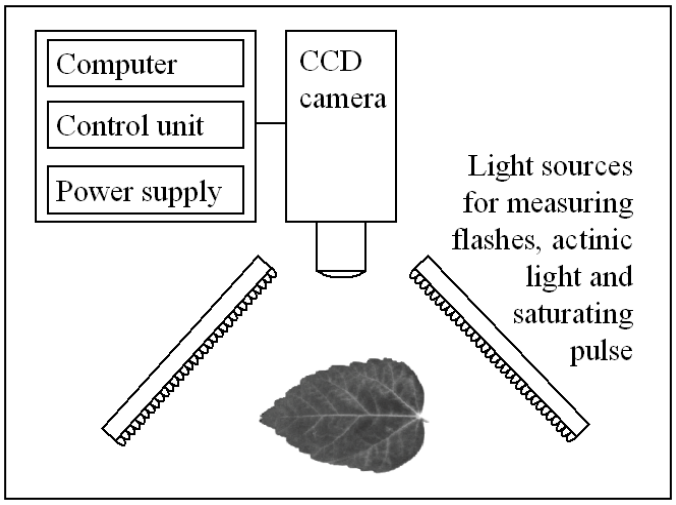

Figure 12. A schematic drawing of a Chl fluorescence imaging instrument showing its key elements. In this configuration, Chl fluorescence emission from a leaf is emitted by arrays of LEDs that generate the measuring light flashes, actinic light, as well as brief intense light pulses (typically 1 s) for measuring F_M and F_M'. The sequence of Chl fluorescence images is captured by a CCD camera equipped with a filter that transmitted red and far-red light (λ > 690 nm). The software allows to design the experimental protocol, and controls the lighting, image capture sequences and further data handling. The experimental protocol is executed by a control unit.

light sources, image capture sequences and further data handling. Nedbal and Whitmarsh [19] have divided the imaging of Chl fluorescence from plants into four basic processes: (i) image capture *i.e.,* illumination, data capture, digitalization, data transfer to a computer; (ii) image segmentation *i.e*., defining the relevant areas or objects for further analysis; (iii) analysis *i.e*., calculation of Chl fluorescence parameters and kinetics for each selected area and object, and (iv) data visualization, which requires calculations of parameters over selected areas that depend on pixel-by-pixel arithmetic operations. The common technique is to visualize the distribution of the Chl fluorescence signal over the selected areas in false scale colors. For this purpose, the black-white scale or the visible spectrum of sunlight is used (where the white or red color represents the highest signal and the black or blue color represents the lowest signal). The spectrum of false scale colors is typically divided into 256 levels (reviewed in [19,20]).

The red Chl fluorescence emission can be recorded together with the blue and green fluorescence (400-630nm) emissions, which primarily arises from hydroxycinnamic acids bound to the cell walls and could reveal effects of various stresses on leaves (*e.g.*, [16,64,155-158]). To increase the reliability of the method, Chl fluorescence imaging can be coupled with nonimaging methods as gas exchange measurement [159], as well as with other imaging techniques

like thermal imaging [17,18,143]. The Chl fluorescence imaging technique can also be coupled with the tools of artificial intelligence [160]. Omasa and Takayama [143] have described an imaging instrument capable of simultaneous measurements of stomatal conductance and Chl fluorescence parameters in intact leaves by both thermal imaging and Chl fluorescence imaging, respectively.

4.2. Applications in plant stress physiology

Chl fluorescence imaging can reveal the internal leaf characteristics that induce heterogeneity in Chl fluorescence emission, *e.g.*, differences in the plant physiology during the life cycle, during day/night cycle as well as the response to variable abiotic and biotic stress factors, both in micro and macro scale (reviewed in [17-21,64]). Here, we present some examples. We have also introduced a number of references to the studies that include data from the Chl fluorescence imaging. References to the early publications are available in [19].

Environmental factors are expected to impact indirectly Chl fluorescence characteristics by the perturbing metabolic pool associated with photosynthetic metabolism. Frequently used Chl fluorescence parameter capable to detect differences in the response of plants to various environmental challenges is Φ_{II} (see the part 3.2.1.). This fluorescence parameter relates to the CO_2 assimilation rate, which is sensitive to a wide range of environmental perturbations, although the sites of limitation of CO_2 assimilation can be quite different. For detailed consequences between the action of environmental stress factors and the decrease in the rate of photosynthesis see, *e.g.*, [119,161]. Nedbal and Whitmarsh [19] described a method to improve estimates of the CO_2 fixation rates over the leaf surface based on Chl fluorescence imaging which requires a map of the quantum yields and a map of the amount of light absorbed by the leaf [162].

Patchiness of the stomata opening or closing is a well-known phenomenon related to differences in photosynthetic activity over the leaf surface caused by differences in CO_2 diffusion into the leaf and internal CO_2 concentration. Thus, Chl fluorescence imaging can be used to distinguish the spatio-temporal variations of the leaf segments that differ in the stomata aperture [138]. Stomata patchiness can be induced by changes in external conditions such as changes in humidity [163,164] and irradiance level [165] or by the change in internal characteristics as concentration of abscisic acid, *etc*. [143,166]. On the cell level, von Craemmerer *et al.* [167] showed that stomatal conductance is not directly determined by the photosynthetic capacity of guard cells or the leaf mesophyll.

Spatio-temporal variability of Φ_{II} occurring during the circadian rhythm over the leaf surface of the CAM plant *Kalanchoe daigremontiana* was revealed by Rascher *et al.* [168]. This patchiness was independent on stomatal control and this independency was explained by lateral CO_2 diffusion and CO_2

signaling in the leaves [169-171]. The potential of lateral diffusion of CO_2 in leaves with different anatomy was investigated by Morison *et al.* [172]. Chl fluorescence imaging together with thermal imaging was used to examine the oscillatory dynamics of stomatal patches after decrease in ambient humidity [164]. Induced oscillation in assimilatory activity were also observed by Siebke and Weis [151,173].

Nedbal and Březina [174] have introduced a new method to visualize the regulation in light capture by revealing images of harmonically forced oscillations in the Chl fluorescence emission. Oscillations can vary in frequencies and/or phases over the leaf surface. The potential of the imaging technology to measure the oscillations in Chl fluorescence was discussed in [19].

Chl fluorescence imaging is employed to reveal also the local effects of drought and high irradiance. Drought stressed leaves reveal heterogeneity particularly in photochemical and nonphotochemical fluorescence quenching (*e.g.*, [175-178]). Gray *et al*. [179] used Chl fluorescence imaging to measure the response of *Arabidopsis thaliana* plants to photoinhibition at low temperature and their subsequent recovery. Similarly, high temperature stress induces the heterogeneity in the Chl fluorescence quenching [9,180,181]. The propagation of a heat-stress signal is proposed to be a result of the electrical signalling in leaves [180]. Lautner *et al.* [182] investigated the electrical signalling in trees using spatio-temporal changes of the quantum yield of PSII photochemistry. Chl fluorescence image analysis is also used as a powerful tool for an early detection of plant stress induced by heavy metal ions [97,183]. The Chl fluorescence imaging technique has further the potential for a rapid screening of perturbations in the plant metabolism caused by herbicides that have both a direct (Fig. 15) (*e.g.*, [19,20,64,139]), and an indirect impact on photosynthesis [184] as well as for assessing the rate of the herbicide microbial degradation [185-187].

The majority of the above mentioned experiments was laboratory-based, with prior dark adaptation of the sample. In some cases (*e.g.,* some field measurements), it is difficult or even impossible to dark adapt the sample prior to the experiment. Thus, only such Chl fluorescence parameters corresponding to the plant LAS can be measured.

Fig. 13 shows an example in which the seasonal changes of Φ_{II} of a spruce tree (*Picea omorica*) was determined under field conditions. Chl fluorescence emission of sun-exposed and shaded shoots was measured *in vivo* using a commercial Chl fluorescence imaging instrument (*Open FluorCam*, Photon Systems Instruments, Czech Republic). Here, sunlight served as the actinic radiation.

In January, photosynthesis in over-wintering shoots is inhibited almost exclusively due to low temperatures. Thus, Φ_{II} values of both shaded and sun-exposed shoots are low ($\Phi_{II} \approx 0.15$). We observed that Φ_{II} rapidly increased during the onset of the vegetation season up to the several fold higher value

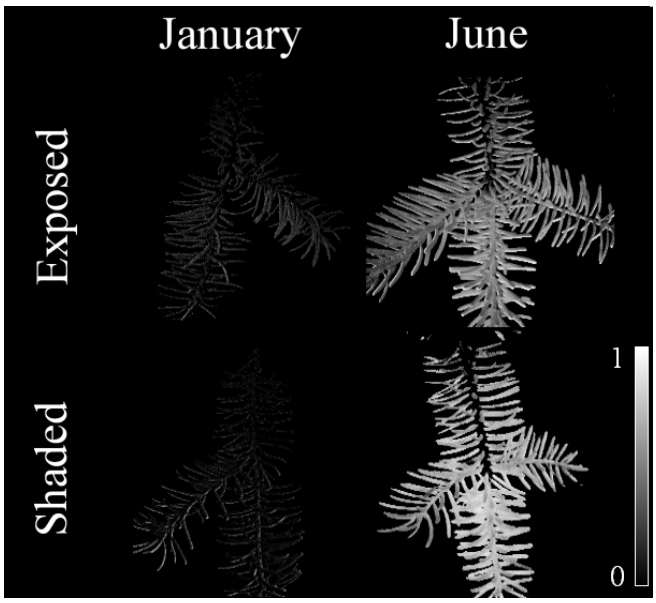

Figure 13. False color Chl fluorescence images of Φ_{II} distribution over a sun-exposed (top row) and shaded (bottom row) shoots of the spruce tree (*Picea omorica*). The tree is located in a park in Nové Hrady (48°47' N, 14°46' E, elevation 541 m a.s.l., SW of the Czech Republic). The Chl fluorescence emission was measured in field conditions under ambient light without any prior dark adaptation on 20th January 2005 and 20th June 2005. Steady state fluorescence (F_S) was determined by short measuring pulses generated by two panels of LEDs ($\lambda \approx 635$ nm), then a 1 s pulse of high intensity radiation (2000 μmol m^{-2} s^{-1}) was given to measure F_M'. Φ_{II} images were calculated pixel-by-pixel using the F_S and F_M' images. Chl fluorescence was detected by a CCD camera that captures the Chl fluorescence images with a resolution of 512x512 pixels. False color scale indicates the Chl fluorescence signal range.

($\Phi_{II} \approx 0.6$ - 0,7) (data not shown). In June, the higher Φ_{II} level was determined in the shaded shoot ($\Phi_{II} \approx 0.7$) than in the sun-exposed shoot ($\Phi_{II} \approx 0.6$). The difference in the photosynthetic activity in sun-exposed and shaded leaves can be explained by the differences in their internal structure and the chlorophyll content (*e.g.*, [158,188]). The distribution of the Chl fluorescence signal along the shoot is homogeneous during the winter period. In summer, Φ_{II} images of the shaded shoot revealed a slight difference between the current year shoots that had a little bit higher Φ_{II} level than the one-year-old shoots. The distribution of Φ_{II} over the sun-exposed shoot was homogeneous.

The Chl fluorescence imaging is frequently used to reveal the photosynthetic heterogeneity caused by the invasion and spreading of various pathogens. It can follow the time course and pathway of pathogen invasion in a leaf. This makes the method an effective tool for an early detection of viral, bacterial and fungal infections of leaves before any visible damage appeared (reviewed in [17,19]). It should be noted that more than a single universal Chl

fluorescence parameter should be used to characterize the evaluation of the pathogen impact [19,189]. The Chl fluorescence response depends on the type of the infection that causes its own distinct influence on the plant metabolism and can vary throughout the progress of the infection. Thereafter, the use of more versatile imaging instruments is recommended.

The effect of biotic stress factors on plant metabolisms is frequently revealed by changes in standard Chl fluorescence parameters that have a known physiological interpretation: F_0, F_M, Φ_{Po}, Φ_{II}, NPQ, *etc*. However, they are not able to reveal all differences of the varying spatial effect induced by the infection. A novel approach in the finding of the most appropriate Chl fluorescence parameters yielding the highest contrast between the healthy and infected plants has been used by Berger *et al.* [189] (see below).

Images of Φ_{II} were used to assay the impact of a fungal pathogen from *Ascochyta rabiei* that altered source-sink distribution on chickpea leaves [190,191]. Similarly, the effect of *Botrytis cinerea* infection on the carbohydrate metabolism in tomato leaves was determined by imaging of changes in Φ_{II} together with NPQ, which likely reflect the plant defense reactions [192]. Also the infection by a mosaic virus was imaged by changes in NPQ [193,194]. Chaerle *et al.* [195] revealed the development of tobacco-mosaic-virus infection in attached tobacco leaves by the combination of the Chl fluorescence imaging with the reflectance and thermography. Onset and progress of defense response of tobacco leaves to a *Phytophtora nicotianae* infection on macro- and micro-scale was imaged also by changes in Φ_{II} [196]. Chl fluorescence imaging was further used to distinguish the hypersensitive and hypersensitive-like response of wild type and mutant of oak to the infection of fungus *Erysiphe cichoracearum* [197]. Further, Zangerl *et al.* [152] and Aldea *et al.* [198] used Chl fluorescence imaging to detect indirect effect of herbivory on plants.

In contrast, rust infection (*Uromyces apendiculatus*) on bean leaves was revealed by changes in the initial phase in the Chl fluorescence induction [199]. Chl fluorescence imaging can be used for assaying and predicting the post-harvest damage in lemons. Images of the F_0/F_V ratio were used to distinguish between the healthy and green mold infected peel areas before the visible symptoms appeared [200]. A simple general experimental algorithm that can be used to identify the Chl fluorescence parameters yielding a high contrast between the treated and non-treated or healthy and infected plant tissue was presented by Soukupová *et al.* [201]. Images of the ratio F_0/F_M as the calculated contrasting parameter were used to visualize the effect of destruxins (phytotoxins of *Alternaria brassicae*) on leaves of canola (*Brassica napus*) and white mustard (*Sinapis alba*).

Here, a similar approach was used to identify the Chl fluorescence markers yielding the highest contrast between the healthy bean plants and bean plants

infected by bacterium *Pseudomonas syringae* (Fig. 14). The contrast is quantified by the discrimination factor, *i.e.*, by the absolute value of the difference between the signals from the control and infected plants divided by the mean square deviation of the signals over the investigated leaf area in control and infected plants. In this experiment, the primary leaves of 15-days-old bean plants were inoculated by a pathogenic bacteria *Pseudomonas syringae*. The infection progress was measured in the primary leaf symmetrical to the inoculated leaf using a Chl fluorescence imaging instrument (*Leaf Chamber FluorCam*, Photon Systems Instruments, Czech Republic). Chl fluorescence emission was excited by six orange high-intensity LEDs providing measuring pulses, actinic radiation, as well as saturating flashes (up to 3000 μmol m^{-2} s^{-1}). One additional light emitting diode ($\lambda \approx 735$nm) selectively excited PS I for F_0' measurement. Chl fluorescence transients were captured from leaf segments (of 2 cm^2) in series of images with a resolution of 512x512 pixels.

To see the early phase of infection, the measurements were taken 3 and 5 days after the inoculation. F_0 and F_M were measured in dark-adapted bean leaves. Then, the leaves were exposed for 100 seconds to the actinic irradiance (90 μmol m^{-2} s^{-1}, $\lambda \approx 635$nm). Two saturating flashes were given at the end of the light period to determine F_M'.

The integrative Chl fluorescence signals (Fig. 14A,B) of infected plants (black circles) differed significantly from controls (white circles) from the 5th day after the infection (see Fig. 14B). No significant difference was seen in the Chl fluorescence transients averaged over the whole measured areas after 3 days (Fig. 14A). On the contrary, the Chl fluorescence imaging revealed clear differences between control and infected leaves at the 3rd day (Fig. 14C). Visible symptoms occurred two weeks after the inoculation (data not shown). The contrast between the Chl fluorescence emission of the infected plants and of the controls is shown by the discrimination factor (triangles in Fig. 14A,B). This contrast between control and infected plants was the strongest typically during the fluorescence decline from the transient maximum level approx. 4 s after the application of the actinic irradiance (F_{24s}). Fig. 14C shows the false-color images, mapping the Chl fluorescence emission over the leaf area of the control (upper panel) and the infected plant (lower panel) after 3 days of infection. No significant variation was seen in the F_0 and Φ_{II} images. The NPQ images revealed a patchy pattern of the Chl fluorescence distribution in the infected leaf. The highest patchiness, clearly distinguished from the homogeneous emission of the control plant, revealed the differential Chl fluorescence image of the infected leaf (the $F_{24s}-F_0$ image).

This example clearly demonstrates that the Chl fluorescence imaging is more powerful in detecting the progress of a pathogen invasion than the

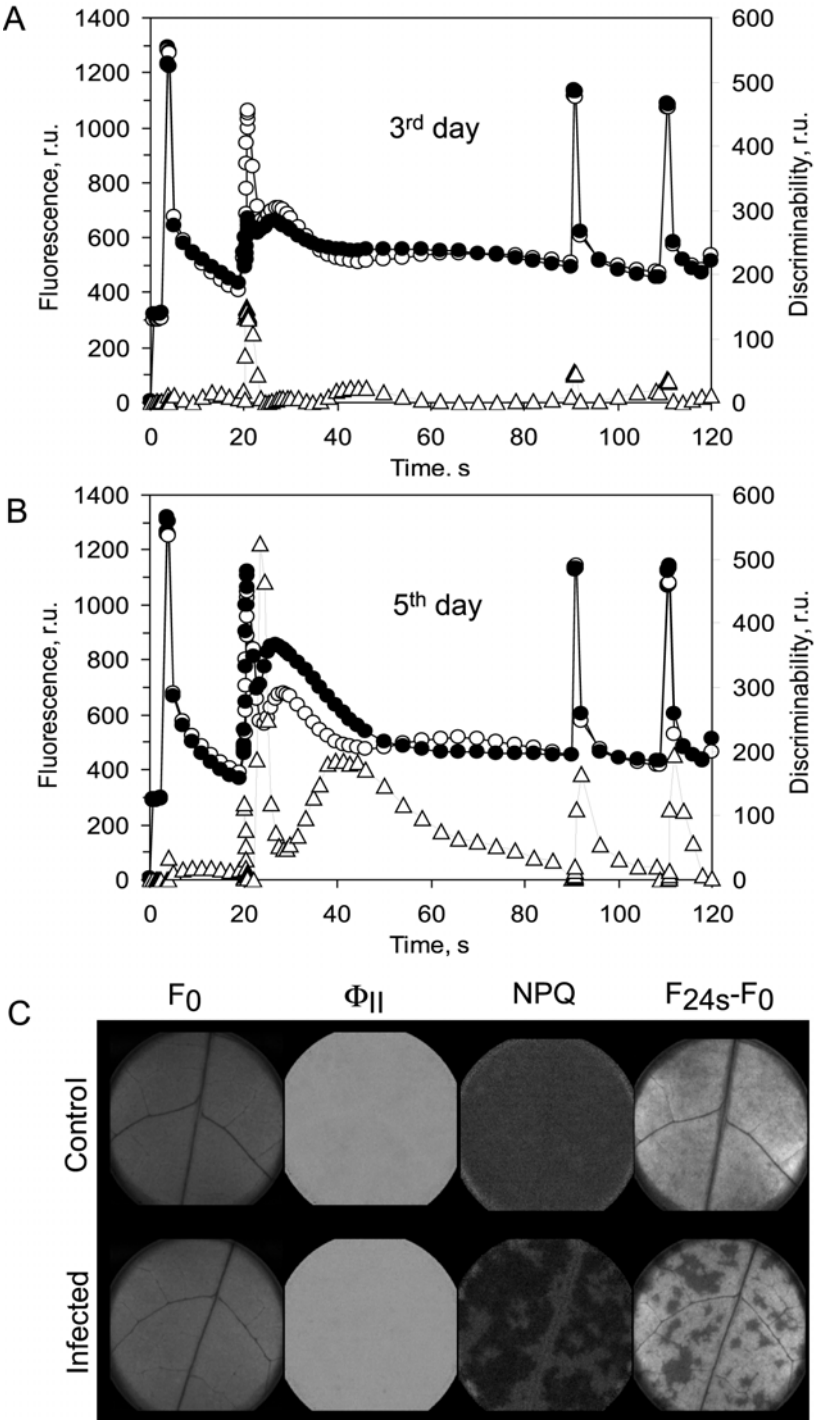

Figure 14. (A) and **(B)** Chl fluorescence transients of healthy bean plants (○) and bean plants infected by bacteria *Pseudomonas syringae* (•) after 3 days **(A)** and 5 days **(B)** of the infection progress. The Chl fluorescence signal was integrated over the entire measured leaf segment areas (2 cm^2). Chl fluorescence was measured first for the dark adapted leaf (F_0). Then, the leaf was illuminated by a 1 s pulse of white saturating light (3000 μmol m^{-2} s^{-1}) for F_M determination. After another dark period, the leaf was exposed

Figure 14. Legend continued

to low actinic light (90 μmol m^{-2} s^{-1}, λ ≈ 635 nm) for 100 seconds. F_M' was determined from the peak Chl fluorescence level reached after the application of a saturation pulse. The contrast between the Chl fluorescence emission of the infected plant and of the control is shown by the discrimination factor (Δ) that reflects both the difference between the averaged fluorescence transients as well as the pixel-to-pixel variability of the signal (see the text for details). **(C)** The false-color images mapping of the Chl fluorescence signal over the leaf area of the control plant (top row) and the infected plant (lower row) after 3 days of infection. No significant variability was seen in F_0 and Φ_{II}. The Chl fluorescence image captured at t = 24 s was calculated to yield the highest contrast between the control and the infected plant (see the discrimination in panels **A** and **B**). This image subtracted by the F_0 value reveals a clear patchiness in the infected leaf. No visual symptom of the infection was observed during the experiment (data not shown).

nonimaging integrative Chl fluorescence technique. The spatiotemporal heterogeneity in Chl fluorescence over the leaf surface requires imaging for its early detection. Moreover, the use of the advanced statistical approaches including the feature selection technique has even higher potential in detecting the combination of Chl fluorescence parameters yielding the highest contrast between the healthy and infected plants. This approach has been described and used by Matouš *et al.* [202] and Berger *et al.* [189]. For a direct comparison to the standard parameters, this evaluation was applied on the infection experiment of *Arabidopsis thaliana* with *Pseudomonas syringae*. The authors demonstrated that an analogous algorithm can be used in various organisms with various pathogens and with the infection monitored by spectral sequences of the images rather than by chronological sequences [189].

Heterogeneity in photosynthetic performance over the leaf occurs even when no stress factor is present. Thus, the Chl fluorescence imaging is well suited to study the evolution of the photosynthetic activity during the leaf development and growth [191,203], senescence and cell death [64,204,205,206]. The heterogeneity in the Chl fluorescence distribution across the leaf during development and growth was attributed to a sucrose metabolism during leaf development [207,208]. Wingler *et al.* [205,206] showed that the processes of leaf senescence and cell death are uncoupled. They proved that the cell death was induced by light-dependent effects causing a photo-oxidative stress and the induction of defence pathways.

The Chl fluorescence can be measured also in plant tissues that have only a limited amount of Chl molecules or exhibit another color than green, as flowers and fruits, because they contain another pigments [85,160,200,209,210]. In food technology, Chl fluorescence has been used to detect perturbations caused by handling and transport of vegetables [211], to determine the optimum O_2 and CO_2 concentrations in modified atmosphere

packages used for their transport [212], and to detect the post-harvest lemon damage [200,213]. The Chl fluorescence imaging technique together with the tools of artificial intelligence were used to classify the quality of harvested apples before storage [160]. The Chl fluorescence imaging has a high potential in increasing both the sensitivity and throughput of plant screening programs in order to identify plants tolerant to environmental stresses, and for improvements in glasshouse production and post-harvest handling of crops, as well (reviewed [161]).

On a microscale, the Chl fluorescence imaging was used to visualize Chl FPs of individual cells or even chloroplasts [140,210,214-220]. It was employed to compare the efficiency of the PSII electron transport in chloroplasts of a guard cell with that in chloroplasts of the underlying mesophyll cells [167]. The photosynthesis of guard and mesophyll cells of various plant species under CO_2, O_2, light or water stress was investigated by Lawson *et al*. [221]. The Chl fluorescence imaging was also used to identify the sites, at which ozone initially induces perturbations of photosynthesis in bean leaves [222]. Goh *et al.* [217] investigated the functional organization of chloroplasts in guard cells of the adaxial and abaxial faces of *Vicia faba* leaves and showed that the photosynthetic apparatus of adaxial guard cells was better adapted to high irradiance levels. Adamec *et al.* [214] monitored the stress-induced filament fragmentation of the cyanobacterium *Calothrix elenkinii*, which was facilitated by the death of cells with high Chl fluorescence yield. Küpper *et al.* [218] investigated the relation between photosynthesis and nitrogen fixation in the marine cyanobacterium *Trichodesmium*. Nitrogen fixation was closely associated with the appearance of cells with high values of F_0. The Chl fluorescence imaging was also used to estimate the rate of photosynthetic electron transport within the biofilms of microbenthic algae [223] and to monitor their primary productivity and the temporal changes in its vertical distribution within the biofilm [224].

4.3. Advantages and limitations of the method

Chl fluorescence imaging can provide 2D-maps of the Chl fluorescence distribution over a photosynthesizing object. It allows to depict the Chl fluorescence parameters over the sample surface, *e.g.* F_0, F_M, F(t), F_0', F_M', and their combinations, that are comparable with that measured by nonimaging instruments (reviewed in [19]). The Chl fluorescence imaging systems enable capturing of thousands of Chl FIKs from a leaf. The captured FIKs can be analyzed individually or integrated into image segments that correspond to individual plants, leaves, leaf segments or cells. These image segments contain detailed information about both the spatial and kinetic heterogeneity of photosynthetic performance over the leaf surface. This feature of Chl

fluorescence imaging systems also allows analysis of a large number of small plants simultaneously.

In comparison with the nonimaging techniques, the capacity to resolve the photosynthetic performance heterogeneity over a plant tissue is the main advantage of the Chl fluorescence imaging. Chl fluorescence can be imaged from the molecular to the plant canopy level. This fact gives the possibility to scale the photosynthetic performance from the sub-cellular to the leaf, and eventually to the field level. Further advantage of recent Chl fluorescence imaging systems is the possibility to capture Chl fluorescence images in direct sunlight under field conditions [139].

The resolving power of Chl fluorescence imaging systems is usually demonstrated by the monitoring inhibition of photosynthesis caused by the herbicide DCMU, a potent inhibitor of the PSII electron transport (*e.g.*, [19,20,64,139]). Fig. 15A shows an example, in which the petiole of detached *Hibiscus* leaf was placed in a 1mM solution of DCMU for 16 hours. As the herbicide is taken up through the transpiration stream, the Chl fluorescence increases around the major veins because the DCMU binds to the Q_B site and blocks the electron transport through RC II [225]. The consequence of the herbicide action is that the energization of the thylakoid membranes is impaired and therefore the nonphotochemical quenching is less efficient than in the absence of the herbicide.

Slow Chl FIK corresponding to the leaf area, in which the photosynthesis was inhibited by DCMU (diamonds in Fig. 15B), was averaged and compared with that of the rest leaf area, where the photosynthesis was not affected (open circles in Fig. 15B). In this experiment, the Chl fluorescence imaging system described in Nedbal *et al.* [139] was used. For comparison, Chl FIK of the whole leaf (black circles) was also averaged. Although the leaf comprised two markedly different areas, the integrative signal only slightly differed from that of the healthy area and did not reveal any significant inhibition.

Although the performance of Chl fluorescence imaging technique has been significantly improved, there still exist some technical limitations. All recent technical limitations have been discussed in details in two recent reviews [19, 20]. The major technical limitations are: (i) the inhomogeneous irradiance (both MR and AR) over a large sample area, and (ii) insufficiently strong and inhomogeneous saturating pulses, which are necessary to reach the maximum Chl fluorescence levels (F_M, F_M'). Consequently, most existing Chl fluorescence imaging systems are limited in a relatively small sample area (up to approximately 100 cm^2), which can be exposed by homogeneous irradiance [19, 20].

The light heterogeneity can impair the distribution of Chl fluorescence signal over the sample area and consequently change the data interpretation. A certain unevenness of MR can be overcome by the calculation of the ratios of fluorescence images, *e.g.* the NPQ parameter, but in this case, details within

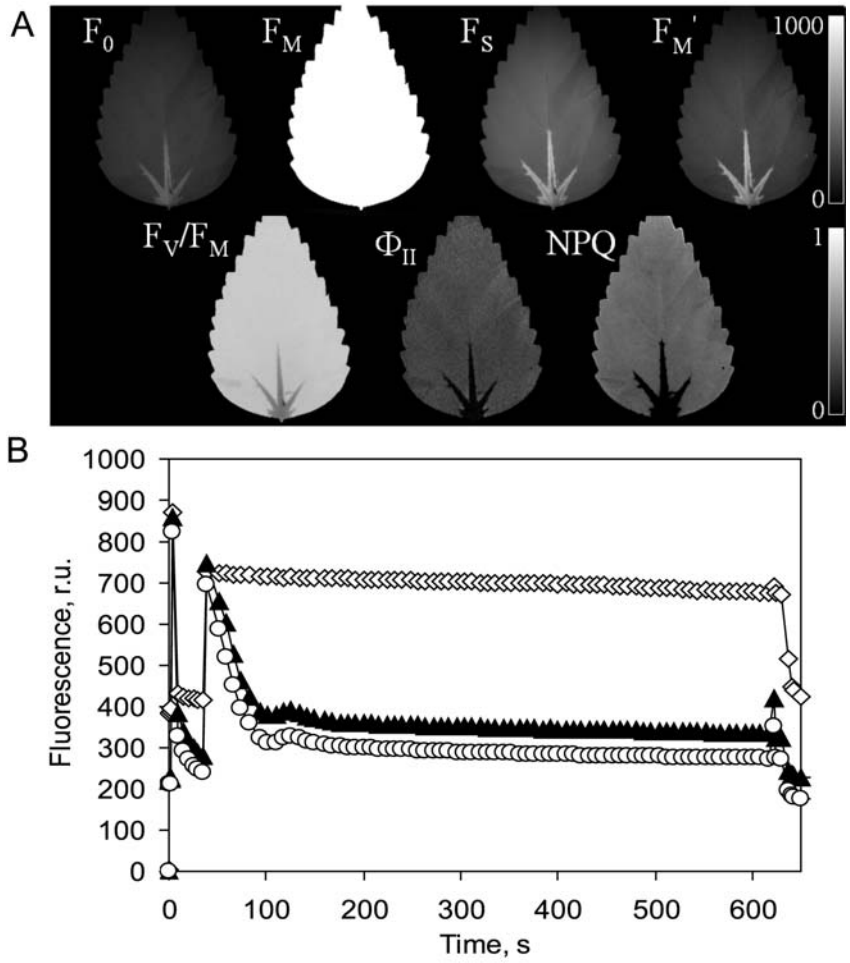

Figure 15. (A) Chl fluorescence images (in a grey scale) showing F_0, F_M, F_S, F_M' (top row), and F_V/F_M, Φ_{II} and NPQ (bottom row) of a detached *Hibiscus* leaf infiltrated by the herbicide DCMU (inhibitor of the PSII electron transport). Chl fluorescence was excited by two panels of LEDs ($\lambda \approx 635$ nm), which provided both the measuring light and actinic illumination. Saturating pulses were generated by a 250W Tungsten™-halogen lamp. Chl fluorescence was detected by a CCD camera that captured the Chl fluorescence transients in series of images with a resolution of 512x512 pixels. Chl fluorescence ratios (bottom row) were calculated pixel-by-pixel using the data from the top row. **(B)** Kinetics of the Chl fluorescence emission from a detached *Hibiscus* leaf partially infiltrated by DCMU calculated from the images shown in Fig. 15A. Slow Chl FIKs were obtained by averaging the signal over the area, where photosynthesis was impaired by DCMU, *i.e.* the leaf area around major veins in the bottom part of the leaf exhibiting higher F_0, F_S and F_M', and lower F_V/F_M, Φ_{II} and NPQ (◊), the area not affected by the herbicide (○), and the whole leaf area (●). After the dark adaptation of the leaf, the F_0 level was measured. Then, the leaf was illuminated by a short (1 s) intensive light pulse (2000 μmol m^{-2} s^{-1}) to determine F_M. After a dark period, the leaf was illuminated by AR (300 μmol m^{-2} s^{-1}, $\lambda \approx 635$ nm) starting at t = 35 s. The F_S level was measured at t = 620 s, then a second saturating pulse was applied to determine F_M'.

original Chl fluorescence images (F_0, F_0', F_M, F(t), F_M') can be lost [19]. This approach, however, cannot be used, if also AR and SPs are not homogenous. For correct recording of F_M images, PFDs from 2000 up to 10000 μmol m^{-2} s^{-1} are required lasting about 1 s [19]. In practice, PFDs used for the F_M imaging are recently in the lower part of this scale.

Introduction of the PAM-principle in Chl fluorescence imaging allowed the accurate imaging of relatively low Chl fluorescence levels, such as F_0 and F_0'. It should be noted that measuring pulses must be widely spaced during the measurement of F_0, so that their actinic effect is minimal [20]. The critical parameter for quantitative analysis is imaging of F_0'. Moreover, not every Chl fluorescence imaging instrument is recently equipped with the far-red illumination that is necessary for the accurate measurement of F_0'. If needed, F_0' image can be calculated using a model developed by Oxborough and Baker [144,226], which is based on measured images of F_0, F_M, and of F_M'.

Considering some technical limitations associated with imaging of F_0, F_0', F_M, and F_M', several strategies were developed to overcome these limitations (reviewed in [19]). For example, F_M has been approximated by F_P measured in rather high, but not saturating AR [227-229]. Similarly, q_N has been estimated from a fixed ratio between F_M and either F_0 or F_0' [173,230]. Ning *et al.* [228] alternated F_0 by F_S measured in low light intensity in given Chl fluorescence parameters. Frequently, the fluorescence decrease ratio $R_{Fd} = (F_M–F_S)/F_M$ (e.g., [39,231,232]) has been used for plant stress (both abiotic and biotic) detection without a necessity to determine the F_0 and F_0' levels.

Besides the technical limitations, biophysical properties of the sample can also limit the usefulness of the technique. They include light scattering, light absorption and re-absorption of Chl fluorescence. All of them are discussed in [19].

5. Concluding remarks

The recording of Chl fluorescence is now well established as a versatile and noninvasive tool for the investigation of the leaf photosynthetic performance under natural conditions. Fluorimetric techniques can reveal a wide range of internal leaf characteristics inducing both spatial and kinetic heterogeneity in the Chl fluorescence emission, including ontogenetic differences in physiological processes occurring during a plant lifetime as well as the plant responses to abiotic and biotic stress factors. Plants have developed many protective and regulatory mechanisms at the chloroplast level to maximize the light energy interception and consequent utilization in the process of CO_2 fixation. As well, numerous mechanisms minimize the light-dependent injury caused to the electron transport chain by over-excitation of the photosynthetic apparatus.

From the explanations given above, it follows that the knowledge of the mechanisms used by photosynthesizing organisms to regulate the excitation energy, is far from being satisfactory. From this point of view, the review brings not only an overview of the well known processes of primary photosynthesis but describes also the technology and methodology of PAM-fluorimetric and Chl fluorescence imaging techniques. The authors tried to demonstrate many advantages and, on the other hand, limitations of these techniques used frequently in the photosynthesis research and plant stress physiology. Because applications of Chl fluorescence recording and imaging are growing rapidly, ranging from basic research at the cell and sub-cellular levels to remote sensing of the plant canopy, the unification in the terminology and a proper use of these powerful tools are necessary. This contribution attempts to support this effort. The intention is also to support and promote the future application of Chl fluorescence techniques both in laboratory and in field studies without technical, instrumental and methodological problems as well as flaws and misinterpretations.

Acknowledgements

This work was supported by the grants Nos. AV0Z 50510513 and IAA600960716 (Institute of Plant Molecular Biology, Biology Centre of the Academy of Sciences of the Czech Republic, p.r.i., České Budějovice, Czech Republik), AV0Z 60870520 (Institute of Systems Biology and Ecology, p.r.i., Academy of Sciences of the Czech Republic, Nové Hrady, Czech Republik), 2004/SP0016 of the Grant Agency of the Academy of Sciences of the Czech Republic, MSM 6007665808 (University of South Bohemia, Institute of Physical Biology, Nové Hrady, Czech Republic) of the Czech Ministry of Education, GACR 522/03/0754 (Masaryk University, Faculty of Science, Brno, Czech Republic) of the Grant Agency of the Czech Republic. J.S. would like to thank Ladislav Nedbal for critical comments, and Ladislav Cséfalvay, Karel Matouš, Matilde Barón and Luis-Rodríguez Moreno for their valuable contributions during experiments.

References

1. Papageorgiou, G.C., and Govindjee 2004, Chlorophyll a Fluorescence: A Signature of Photosynthesis, Springer, Dordrecht.
2. Walker, D. 1987, The Use of the Oxygen Electrode and Fluorescence Probes in Simple Measurements of Photosynthesis, D. Walker (Ed.), Univ. of Sheffield, Sheffield, 17.
3. Govindjee 1995, Aust. J. Plant Physiol., 22, 131.
4. Govindjee 2004, Chlorophyll a Fluorescence: A Signature of Photosynthesis, G.C. Papageorgiou, and Govindjee (Eds.), Springer, Dordrecht, 1.
5. Krause, G.H., and Weis, E. 1991, Annu. Rev. Plant Physiol. Plant Mol. Biol., 42, 313.

6. Lazár, D. 1999, Biochim. Biophys. Acta, 1412, 1.
7. Lazár, D. 2006, Functional Plant Biol., 33, 9.
8. Maxwell, K., and Johnson, G.N. 2000, J. Exp. Bot., 51, 659.
9. Schreiber, U. 2004, Chlorophyll a Fluorescence: A Signature of Photosynthesis, G.C. Papageorgiou, and Govindjee (Eds.), Springer, Dordrecht, 279.
10. Schreiber, U. 1986, Photosynth. Res., 9, 261.
11. Schreiber, U., Schliwa, U., and Bilger, W. 1986, Photosynth. Res., 10, 51.
12. Adams III, W.W., and Demmig-Adams, B. 2004, Chlorophyll a Fluorescence: A signature of Photosynthesis, G.C. Papageorgiou, and Govindjee (Eds.), Springer, Dordrecht, 583.
13. Bukhov, N.G., and Carpentier, R. 2004, Chlorophyll a Fluorescence: A signature of Photosynthesis, G.C. Papageorgiou, and Govindjee (Eds.), Springer, Dordrecht, 623.
14. Lichtenthaler, H.K. 1990, Applications of Remote Sensing in Agriculture, M.D. Steven, and J.A. Clark (Eds.), Butterworth-Heinemann, Stoneham, 287.
15. Šiffel, P., and Vácha, F. 1998, Photochem. Photobiol., 67, 304.
16. Buschmann, C., Langsdorf, G., and Lichtenthaler, H.K. 2000, Photosynthetica, 38, 483.
17. Chaerle, L., and van der Straeten, D. 2000, Trends Plant Sci., 5, 495.
18. Chaerle, L., and van der Straeten, D. 2001, Biochim. Biophys. Acta - Gene Struct. Expr., 1519, 153.
19. Nedbal, L., and Whitmarsh, J. 2004, Chlorophyll a Fluorescence: A Signature of Photosynthesis, G.C. Papageorgiou, and Govindjee (Eds.), Springer, Dordrecht, 389.
20. Oxborough, K. 2004, Chlorophyll a Fluorescence: A signature of Photosynthesis, G.C. Papageorgiou, and Govindjee (Eds.), Springer, Dordrecht, 409.
21. Moya, I., and Cerovic, Z.G. 2004, Chlorophyll a Fluorescence: A signature of Photosynthesis, G.C. Papageorgiou, and Govindjee (Eds.), Springer, Dordrecht, 429.
22. Gavel, A., and Maršálek, B. 2004, Environ. Toxicol., 19, 429.
23. Gower, J.F.R., and Borstad, G.A. 2004, Int. J. Remote Sens., 25, 1459.
24. Voet, D., and Voet, J.G. 2005, Biochemistry, 3rd edition, John Wiley and Sons, 1616.
25. Standfuss, J., Terwisscha van Scheltinga, A.C., Lamborghini, M., and Kühlbrandt, W. 2005, EMBO J., 24, 919.
26. Webber, A.N., and Baker, N.R. 1996, Oxygenic Photosynthesis: The Light Reactions, D.R. Ort, and C.F. Yocum (Eds.), Kluwer, Dordrecht, 41.
27. Adams, W.W., Demmig-Adams, B., Verhoeven, A.S., and Barker, D.H. 1995, Aust. J. Plant Physiol., 22, 261.
28. Buffoni, M., Testi, M.G., Pesaresi, P., Garlaschi, F.M., and Jennings, R.C. 1998, Physiol. Plant., 102, 318.
29. Demmig-Adams, B., and Adams W.W. 1996, Trends Plant Sci., 1, 21.
30. Schreiber, U., Bilger, W., and Neubauer, C. 1995, Ecophysiology of Photosynthesis, E.-D. Schulze, and M.M. Caldwell (Eds.), Springer, Berlin, Heidelberg, 49.
31. Demmig-Adams, B., Adams III, W.W., Barker, D.H., Logan, B.A., Bowling, D.R., and Verhoeven, A.S. 1996, Physiol. Plant., 98, 253.

32. Papageorgiou, G. 1975, Bioenergetics of Photosynthesis, Govindjee (Ed.), Academic Press, New York, London, 319.
33. Govindjee, and Govindjee, R. 1975, Bioenergetics of Photosynthesis, Govindjee (Ed.), Academic Press, New York, London, 1.
34. Roháček, K. 2002, Photosynthetica, 40, 13.
35. Buschmann, C. 1995, Photosynthesis: From Light to Biosphere, P. Mathis (Ed.), Vol. V, Kluwer, Dordrecht, 913.
36. Kautsky, H., and Hirsch, A. 1931, Naturwissenschaften 19, 964.
37. Kautsky, H., and Hirsch, A.1934, Biochem. Z., 274, 423.
38. Bradbury, M., and Baker, N.R. 1981, Biochim. Biophys. Acta, 635, 542.
39. Lichtenthaler, H.K., Buschmann, C., Rinderle, U., and Schmuck, G. 1986, Radiat. Environ. Biophys., 25, 297.
40. Strasser, R.J., Tsimilli-Michael, M., and Srivastava, A. 2004, Chlorophyll a Fluorescence: A Signature of Photosynthesis, G.C. Papageorgiou, and Govindjee (Eds.), Springer, Dordrecht, 321.
41. Zhu, X.-G., Govindjee, Baker, N.R., deSturler, E., Ort, D.R., and Long, S.P. 2005, Planta, 223, 114.
42. Buschmann, C., and Prehn, H. 1990, Modern Methods of Plant Analysis, New Series, Vol. 11, Physical Methods in Plant Sciences, H.F. Linskens, and J.F. Jackson (Eds.), Springer, Berlin, 148.
43. Malkin, S. 1996, Biophysical Techniques in Photosynthesis, J. Amesz, and A.J. Hoff (Eds.), Kluwer, Dordrecht, 191.
44. Mullineaux, C.W. 1993, Biochim. Biophys. Acta 1143, 235.
45. Tabrizi, H., Schinner, K., Spors, J., and Hansen, U.-P. 1998, Photosynth. Res., 57, 101.
46. Fork, D.C., and Herbert, S.K. 1993, Photochem. Photobiol. 57, 207.
47. van Kooten, O., and Snel, J.F.H. 1990, Photosynth. Res., 25, 147.
48. Björkman, O., and Demmig-Adams, B. 1995, Ecophysiology of Photosynthesis, E.-D. Schulze, and M.M. Caldwell (Eds.), Springer, Berlin, 17.
49. Ruban, A.V., Lavaud, J., Rousseau, B., Guglielmi, G., Horton, P., and Etienne, A.-L. 2004, Photosynth. Res., 82, 165.
50. Barber, J. 1995, Aust. J. Plant Physiol., 22, 201.
51. Havaux, M., and Davaud, A. 1994, Photosynth. Res., 40, 92.
52. Pospíšil, P. 1997, Photosynthetica, 34, 343.
53. Gilmore, A.M., and Yamamoto, H.Y. 1993, Photosynth. Res., 35, 67.
54. Jahns, P., and Krause, G.H. 1994, Planta, 192, 176.
55. Ruban, A.V., and Horton, P. 1995, Aust. J. Plant Physiol., 22, 221.
56. Schreiber, U., Klughammer, C., and Neubauer, C. 1988, Z. Naturforsch., 43c, 686.
57. Roháček, K., and Barták, M. 1999, Photosynthetica, 37, 339.
58. Schreiber, U., Neubauer, C., and Schliwa, U. 1993, Photosynth. Res., 36, 65.
59. Bradbury, M., and Baker, N.R. 1984, Biochim. Biophys. Acta, 765, 275.
60. Selye, H. 1936, Nature, 138, 32.
61. Lichtenthaler, H.K. 1998, Stress of Life: From Molecules to Man, P. Csermely (Ed.), Annals of the N.Y. Acad. Sci., 851, CDP/PCP, New York, 187.
62. Hasegava, P.M. 1998, Plant Physiology, L. Taiz, and E. Zeiger (Eds.), Sinauer Associates, Inc., Sunderland, 725.
63. Larcher, W. 1987, Naturwissenschaften, 74, 158.

64. Lichtenthaler, H.K., and Babani, F. 2004, Chlorophyll a Fluorescence: A signature of Photosynthesis, G.C. Papageorgiou, and Govindjee (Eds.), Springer, Dordrecht, 713.
65. Strasser, R.J., and Govindjee 1992, Regulation of Chloroplast Biogenesis, J.H. Argyroudi-Akoyungolou (Ed.), Plenum Press, New York, 423.
66. Strasser, R.J., and Tsimilli-Michael, M. 1998, Photosynthesis: Mechanisms and Effects, G. Garab (Ed.), Kluwer, Dordrecht, 4321.
67. Pospíšil, P., and Dau, H. 2002, Biochim. Biophys. Acta, 1554, 94.
68. Tsimilli-Michael, M., Pêcheux, M., and Strasser, R.J. 1998, Photosynthesis: Mechanisms and Effects, G. Garab (Ed.), Kluwer, Dordrecht, 4113.
69. Srivastava, A., and Strasser, R.J. 1996, J. Plant Physiol., 148, 445.
70. Bussotti, F., Agati, G., Desotgiu, R., Matteini, P., and Tani, C. 2005, New Phytol., 166, 941.
71. van Rensburg, L., Krüger, G.H.J., Eggenberg, P., and Strasser, R.J. 1996, South Afr. J. Bot., 62, 337.
72. Lazár, D., Nauš, J., Matoušková, M., and Flašarová, M. 1997, Pesticides Biochem. Physiol., 57, 200.
73. Barták, M. 2000, Topics in Ecology. Structure and Function in Plants and Ecosystems, R. Ceulemans, J. Bogaert, G. Deckmyn, and I. Nijs (Eds.), Univ. Antwerp, 211.
74. Tsimilli-Michael, M., Pêcheux, M., and Strasser, R.J. 1999, Z. Naturforsch., 54c, 671.
75. Hill, R., Larkum, A.W.D., Frankart, C., Kuhn, M., and Ralph, P.J. 2004, Photosynth. Res., 82, 59.
76. Bukhov, N.G., Egorova, E.A., Govindachary, S., and Carpentier, R. 2004, Biochim. Biophys. Acta, 1657, 130.
77. Ilík, P., Schansker, G., Kotabová, E., Váczi, P., Strasser, R., and Barták, M. 2006, Biochim. Biophys. Acta – Bioenergetics, 1757, 12.
78. Stirbet, A., Govindjee, Strasser, B.J., and Strasser, R.J. 1998, J. Theor. Biol., 193, 131.
79. Lazár, D., and Pospíšil, P. 1999, Europ. Biophys. J., 82, 468.
80. Lazár, D., Tomek, P., Ilík, P., and Nauš, J. 2001, Photosynth. Res., 68, 247.
81. Lazár, D., and Ilík, P. 1997, Plant Sci., 124, 159.
82. Lazár, D. 2003, J. Theor. Biol., 220, 469.
83. Strasser, R.J., and Stirbet, A.D. 2001, Math. Comp. Simul., 56, 451.
84. Reigosa Roger, M.J., and Weiss, O. 2001, Handbook of Plant Ecophysiology Techniques, M.J. Reigosa Roger (Ed.), Kluwer, Dordrecht, 155.
85. Schoefs, B. 2002, Trends Food Sci. Technol., 13, 361.
86. Horton, P, and Hague, A 1988, Biochim. Biophys. Acta, 932, 107.
87. Hodges, M., Cornic, G., and Briantais, J.-M. 1989, Biochim. Biophys. Acta, 974, 289.
88. Krause, G.H., and Jahns, P. 2004, Chlorophyll a Fluorescence: A Signature of Photosynthesis, G.C. Papageorgiou, and Govindjee (Eds.), Springer, Dordrecht, 463.
89. Bilger, W., and Björkman, O. 1990, Photosynth. Res., 25, 173.
90. Quick, W.P., and Stitt, M. 1990, Biochim. Biophys. Acta, 977, 287.
91. Bruce, D., and Vasil'ev, S. 2004, Chlorophyll a Fluorescence: A signature of Photosynthesis, G.C. Papageorgiou, and Govindjee (Eds.), Springer, Dordrecht, 497.

92. Laisk, A., and Oja, V. 1998, Dynamics of Leaf Photosynthesis, A. Laisk, and V. Oja (Eds.), CSIRO Publ., Collingwood, Australia, 64.
93. Stitt, M., Huber, S., and Kerr P. 1987, The Biochemistry of Plants, P.K. Stumpf, and E.E. Conn (Eds.), Academic Press, San Diego, London, 327.
94. Lichtenthaler, H.K., Buschmann, C., and Knapp M. 2005, Photosynthetica, 43, 379.
95. Kitajima, M., and Butler, W.L. 1975, Biochim. Biophys. Acta, 376, 105.
96. Björkman, O., and Demmig, B. 1987, Planta, 170, 489.
97. Joshi, M.K., and Mohanty, P. 2004, Chlorophyll a Fluorescence: A signature of Photosynthesis, G.C. Papageorgiou, and Govindjee (Eds.), Springer, Dordrecht, 637.
98. Lavergne, J., and Trissl, H.-W. 1995, Biophys. J., 68, 2474.
99. Pfündel, E. 1998, Photosynth. Res., 56, 185.
100. Franck, F., Juneau, P., and Popovic, R. 2002, Biochim. Biophys. Acta - Bioenerg., 1556, 239.
101. Duysens, L.N.M., and Sweers, H.E. 1963, Studies on Microalgae and Photosynthetic Bacteria, J. Ashida (Ed.), Plant Cell Physiol., Spec. Issue, Univ. Tokyo, Tokyo, 353.
102. Krause, G.H., Vernotte, C., and Briantais, J.-M. 1982, Biochim. Biophys. Acta, 679, 116.
103. Bilger, W., and Schreiber, U. 1986, Photosynth. Res., 10, 303.
104. Genty, B., Wonders, J., and Baker, N.R. 1990, Photosynth. Res., 26, 133.
105. Horton, P., and Ruban, A.V. 1992, Photosynth. Res., 34, 375.
106. Rees, D., Noctor, G.D., and Horton, P. 1990, Photosynth. Res., 25, 199.
107. Gilmore, A.M. 2004, Chlorophyll a Fluorescence: A signature of Photosynthesis, G.C. Papageorgiou, and Govindjee (Eds.), Springer, Dordrecht, 555.
108. Horton, P. 1996, Light as an Energy Source and Information Carrier in Plant Physiology, R.C. Jennings, G. Zucchelli, F. Ghetti, and G. Colombetti (Eds.), NATO ASI Ser. A: Life sciences, Vol. 287, Plenum Press, New York, London, 99.
109. Genty, B., Briantais, J.-M., and Baker, N.R. 1989, Biochim. Biophys. Acta, 990, 87.
110. Walters, R.G., and Horton, P. 1991, Photosynth. Res., 27, 121.
111. Lichtenthaler, H.K., and Burkart, S. 1999, Bulg. J. Plant Physiol., 25, 3.
112. Kramer, D.M., and Crofts, A.R. 1996, Photosynthesis and the Environment, N.R. Baker (Ed.), Kluwer, Dordrecht, 25.
113. Lee, C.B., Rees, D., and Horton, P. 1990, Photosynth. Res., 24, 167.
114. Durchan, M., Vácha, F., and Krieger-Liszkay, A. 2001, Photosynth. Res., 68, 203.
115. Havaux, M., and Niyogi, K.K. 1999, Proc. Natl. Acad. Sci. USA, 96, 8762.
116. Bertrand, M., and Poirier, I. 2005, Photosynthetica, 43, 345.
117. Mullineaux, C.W., and Allen, J.F. 1990, Photosynth. Res. 23, 297.
118. Allen, J.F., and Mullineaux, C.W. 2004, Chlorophyll a Fluorescence: A signature of Photosynthesis, G.C. Papageorgiou, and Govindjee (Eds.), Springer, Dordrecht, 447.
119. Baker, N.R., and Oxborough, K. 2004, Chlorophyll a Fluorescence: A signature of Photosynthesis, G.C. Papageorgiou, and Govindjee (Eds.), Springer, Dordrecht, 65.
120. Cavender-Bares, J., and Bazzaz, F.A. 2004, Chlorophyll a Fluorescence: A signature of Photosynthesis, G.C. Papageorgiou, and Govindjee (Eds.), Springer, Dordrecht, 737.

121. Schoefs, B. 2005, Photosynthetica, 43, 329.
122. Bertrand, M., Schoefs, B., Siffel, P., Rohacek, K., and Molnar, I. 2001, FEBS Lett., 508, 153.
123. Roháček, K., and Šiffel, P. 1995, Photosynthesis: From Light to Biosphere, P. Mathis (Ed.), Vol. V., Kluwer, Dordrecht, 937.
124. Cornic, G., and Massacci, A. 1996, Photosynthesis and the Environment, N.R. Baker (Ed.), Kluwer, Dordrecht, 347.
125. Pospíšilová, J. 2003, Biol. Plant., 46, 491.
126. Šantrůček, J., Hronková, M., Květoň, J., and Sage, R.F. 2003, Photosynthetica, 41, 241.
127. Raven, J.A. 1995, Ecophysiology of Photosynthesis, E.-D. Schulze, and M.M. Caldwell (Eds.), Springer, Berlin, Heidelberg, 299.
128. Prášil, O., Adir, N., and Ohad, I. 1992, The Photosystems: Structure, Function and Molecular Biology, J. Barber (Ed.), Elsevier, Amsterdam, 295.
129. Adamska, I. 1997, Physiol. Plant., 100, 794.
130. Baker, N.R 1996, Light as an Energy Source and Information Carrier in Plant Physiology, R.S. Jennings, G. Zucchelli, F. Ghetti, and G. Colombetti (Eds.), NATO ASI Series A, Plenum Press, New York, London, 89.
131. Eskling, M., Arvidsson, P.-O., and Åkerlund, H.-E. 1997, Physiol. Plant., 100, 806.
132. Bilger, W., Schreiber, U., and Lange, O.L. 1987, Plant Response to Stress, J.D. Tenhunen, F.M. Catarino, O.L. Lange, and W.C. Oechel (Eds.), Springer, Berlin, Heidelberg, 391.
133. Lazár, D., Kaňa, R., Klinkovský, T., and Nauš, J. 2005, Photosynthetica, 43, 13.
134. Gilmore, A.M. 1997, Physiol. Plant., 99, 197.
135. Ghashghaie, J., and Cornic, G. 1994, J. Plant Physiol., 143, 643.
136. Georgieva, K., and Yordanov, I. 1994, J. Plant Physiol., 144, 754.
137. Omasa, K., Shimazaki, K., Aiga, I., Laracher, W., and Onoe, M. 1987, Plant Physiol., 84, 748.
138. Daley, P., Raschke, K., Ball, J., and Berry, J. 1989, Plant Physiol. 90, 1233.
139. Nedbal, L., Soukupová, J., Kaftan, D., Whitmarsh, J., and Trtílek, M. 2000, Photosynth. Res., 66, 3.
140. Küpper, H., Šetlík, I., Trtílek, M., and Nedbal, L. 2000, Photosynthetica, 38, 553.
141. Govindjee, and Nedbal, L. 2000, Photosynthetica, 38, 481.
142. Grunwald, B., and Kuhl, M. 2004, Ophelia, 58, 79.
143. Omasa, K., and Takayama, K. 2003, Plant Cell Physiol., 44, 1290.
144. Oxborough, K., and Baker, N. 1997, Photosynth. Res., 54, 135.
145. Osmond, C., Schwartz, O., and Gunning, B. 1999, Aust. J. Plant Physiol., 26, 717.
146. Rolfe, S.A., and Scholes, J.D. 2002, Photosynth. Res., 72, 107.
147. Fenton, J., and Crofts, A. 1990, Photosynth. Res., 26, 59.
148. Genty, B., and Meyer, S. 1995, Austr. J. Plant Physiol., 22, 277.
149. Lootens, P., and Vandecasteele, P. 2000, Photosynthetica, 38, 53.
150. Scholes, J., and Rolfe, S. 1996, Planta, 199, 573.
151. Siebke, K., and Weis, E. 1995, Photosynth. Res., 45, 225.
152. Zangerl, A.R., Hamilton, J.G., Miller, T.J., Crofts, A.R., Oxborough, K., Berenbaum, M.R., and de Lucia, E.H. 2002, Proc. Nat. Acad. Sci. USA, 99, 1088.
153. Nedbal, L., and Koblížek, M. 2005, Biochemistry and Biophysics of Chlorophylls, B. Grimm, R. Porra, W. Rüdiger, and H. Scheer (Eds.), Kluwer, Dordrecht, In press.

154. Nedbal, L., Trtílek, M., and Kaftan, D. 1999, J. Photochem. Photobiol. B, 48, 154.
155. Buschmann, C., and Lichtenthaler, H.K. 1998, Plant Physiol., 152, 297.
156. Corp, L.A., McMurtrey, J.E., Middleton, E.M., Mulchi, C.L., Chappelle, E.W., and Daughtry, C.S.T. 2003, Remote Sensing Environ., 86, 470.
157. Langsdorf, G., Buschmann, C., Sowinska, M., Babani, F., Mokry, M., Timmermann, F., and Lichtenthaler, H.K. 2000, Photosynthetica, 38, 539.
158. Lichtenthaler, H.K., Lang, M., Sowinska, M., Heisel, F., and Miehe, J. 1996, J. Plant Physiol., 148, 599.
159. Lawson, T., Oxborough, K., Morison, J.I.L., and Baker, N.R., 2002, Plant Physiol. 128, 1.
160. Codrea, M.C., Nevalainen, O.S., Tyystjärvi, E., Vandeven, M., and Valcke, R. 2004, Int. J. Pattern Recogn. Artif. Intellig., 18, 157.
161. Baker, N.R., and Rosenquist, E. 2004, J. Exp. Bot. 55, 1607.
162. Krall, J., and Edwards, G. 1992, Physiol. Plant., 86, 180.
163. Meyer, S., and Genty, B. 1999, Planta 210, 126.
164. West, J.D., Peak, D., Peterson, J.Q., and Mott, K.A. 2005, Plant Cell Environ. 28, 633.
165. Eckstein, J., Beyschlag, W., Mott, K., and Ryel, R. 1996, Plant Cell, 19, 1066.
166. Meyer, S., and Genty, B. 1998, Plant Physiol., 116, 947.
167. von Craemmerer, S., Lawson, T., Oxborough, K., Baker, N.R., Andrews, T.J., and Raines C.A. 2004, J. Exp. Bot., 55, 1157.
168. Rascher, U., Hütt, M.-T., Siebke, K., Osmond, B., Beck, F., and Lüttge, U. 2001, Proc. Natl. Acad. Sci. USA, 98, 11801.
169. Duarte, H.M., Jakovljevic, I., Kaiser, F., and Lüttge, U. 2005, Planta, 220, 809.
170. Maddess, T., Rascher, U., Siebke, K., Lüttge, U., and Osmond, B. 2002, Plant Biol., 4, 446.
171. Rascher, U., and Lüttge, U. 2002, Plant Biol., 4, 671.
172. Morison, J.I.L., Gallouet, E., Lawson, T., Cornic, G., Herbin, R., and Baker, N.R. 2005, Plant Physiol., 139, 254.
173. Siebke, K., and Weis, E. 1995, Planta, 196, 155.
174. Nedbal, L., and Březina, V. 2002, Biophys. J., 83, 2180.
175. Barták, M., Hájek, J., and Gloser, J. 2000, Photosynthetica, 38, 531.
176. Barták, M., Hájek, J., Vráblíková, H., and Dubová, J. 2004, Plant Biol., 6, 333.
177. Barták, M., Gloser, J., and Hájek, J. 2005, Lichenologist, 37, 433.
178. Lichtenthaler, H.K., Babani, F., Langsdorf, G., and Buschmann, C. 2000, Photosynthetica, 38, 521.
179. Gray, G.R., Hope, B.J., Qin, X., Taylor, B.G., and Whitehead, C.L. 2003, Physiol. Plant., 119, 365.
180. Koziolek, C., Grams, T.E.E., Schreiber, U., Matyssek, R., and Fromm, J. 2003, New Phytol., 161, 715.
181. Schreiber, U., Walz, H., and Kolbowski, J. 2003, http://www.pam-news.de/ar/03-01/PAMNews03-01.html (June 22).
182. Lautner, S., Grams, T.E.E., Matyssek, R., and Fromm, J. 2005, Plant Physiol., 138, 2200.
183. Ciscato, M., and Valcke, R. 1998, Photosynthesis: Mechanisms and Effects, G. Garab (Ed.), Vol. IV, Kluwer, Dordrecht, 2661.

184. Barbagallo, R.P., Oxborough, K., Pallett, K.E., and Baker, N.R. 2003, Plant Physiol., 132, 485.
185. Chaerle, L., Hulsen, K., Hermans, C., Strasser, R.J., Valcke, R., Hofte, M., and van der Straeten, D. 2003, Physiol. Plant., 118, 613.
186. Hulsen, K., Top, E.M., and Höfte, M. 2002, New Phytol., 154, 821.
187. Hulsen, K., Minne, V., Lootens, P., Vandecasteele, P., and Höfte, M. 2002, Environ. Microbiol., 4, 327.
188. Lichtenthaler, H.K., Buschmann, C., Döll, M., Fietz, H.-J., Bach, T., Kozel, U., Meier, D., and Rahmsdorf, U. 1981, Photosynth. Res., 2, 115.
189. Berger, S., Benediktyová, Z., Matouš, K., Bonfig, K., Mueller, M.J., Nedbal, L., and Roitsch, T. 2007, J. Exp. Bot., 58, 797.
190. Esfeld, P., Siebke, K., Wacker, I., and Weis, E. 1995, Photosynthesis: From Light to Biosphere, P. Mathis (Ed.), Kluwer, Dordrecht, 663.
191. Weis, E., Meng, Q., Siebke, K., Lippert, K., and Esfeld, P. 1998, Photosynthesis: Mechanisms and Effects, G. Garab (Ed.), Kluwer, Dordrecht, 4259.
192. Berger, S., Papadopoulos, M., Schreiber, U., Kaiser, W., and Roitsch, T. 2004, Physiol. Plant., 122, 419.
193. Lohaus, G., Heldt, H., and Osmond, C. 2000, Plant Biol., 2, 161.
194. Osmond, C., Daley, P., Badger, M., and Lüttge, U. 1998, Bot. Acta, 111, 390.
195. Chaerle, L., Hagenbeek, D., De Bruyne, E., Valcke, R., and van der Straeten, D. 2004, Plant Cell Physiol., 45, 887.
196. Scharte, J., Schön, H., and Weis, E. 2005, Plant Cell Environ., 28, 1421.
197. Repka, V. 2002, Photosynthetica, 40, 183.
198. Aldea, M, Hamilton, J.G., Resti, J.P., Zangerl, A.R., Berenbaum, M.R., and deLucia, E.H. 2005, Plant Cell Environ., 28, 402.
199. Peterson, R., and Aylor, D. 1995, Plant Physiol., 108, 163.
200. Nedbal, L., Soukupová, J., Whitmarsh, J., and Trtílek, M. 2000, Photosynthetica, 38, 573.
201. Soukupová, J., Smatanová, S., Nedbal, L., and Jegorov, A. 2003, Physiol. Plant., 118, 1.
202. Matouš, K., Benediktyová, Z., Berger, S., Roitsch, T., and Nedbal, L. 2006, Photosynth. Res., 90, 243.
203. Croxdale, J., and Omasa, K. 1990, Plant Physiol., 93, 1083.
204. Oh, M.H., Kim, Y.J., and Lee, C.W. 2000, J. Biochem. Mol. Biol., 33, 256.
205. Wingler, A., Mares, M., and Pourtau, N. 2004, New Phytol., 161, 781.
206. Wingler, A., Brownhill, E., and Pourtau, N. 2005, J. Exp. Bot., 56, 1.
207. Meng, Q., Siebke, K., Lippert, P., Baur, B., Mukherjee, U., and Weis, E. 2001, New Phytol., 151, 585.
208. Walter, A., Rascher, U., and Osmond, B. 2004, Plant Biol., 6, 184.
209. Bodria, L., Fiala, M., Guidetti, R., and Oberti, R. 2004, Transactions ASAE, 47, 815.
210. Zangerl, A., Berenbaum, M.R., DeLucia, E.H., and Nitao, J.K. 2003, Ecology Lett., 6, 966.
211. DeEll, J.R., and Toivonen, M.P.A., 2003, Practical Applications of Chlorophyll Fluorescence in Plant Biology, J.R. DeEll, and P.M.A. Toivonen (Eds.), Kluwer, Boston, 201.
212. Toivonen, P.M.A., and DeEll, J.R. 2001, Post-harvest Biol. Technol., 23, 61.

213. Obenland, D., and Neipp, P. 2005, Hortscience, 40, 1821.
214. Adamec, F., Kaftan, D., and Nedbal, L. 2005, J. Phycol., 41, 835.
215. Baker, N., Oxborough, K., Lawson, T., and Morison, J. 2001, J. Exp. Bot., 52, 615.
216. Ferimazova, N., Küpper, H., Nedbal, L., and Trtílek, M. 2002, Photochem. Photobiol., 76, 501.
217. Goh, C.H., Hedrich, R., Nam, H.G. 2002, Plant Sci., 162, 965.
218. Küpper, H., Ferimazova, N., Šetlík, I., and Berman-Frank, I. 2004, Plant Physiol., 135, 2120.
219. Oxborough, K., Hanlon, A.R.M., Underwood, G.J.C., and Baker, N.R. 2000, Limnol. Oceanogr., 45, 1420.
220. Šetlíková, E., Šetlík, I., Küpper, H., Kasalický, V., and Prášil, O. 2005, Photosynth. Res., 84, 113.
221. Lawson, T., Oxborough, K., Morison, J.I., and Baker, N.R. 2003, J Exp. Bot., 54, 1743.
222. Leipner, J., Oxborough, K., and Baker, N.R. 2001, J. Exp. Bot., 52, 1689.
223. Perkins, R.G., Oxborough, K., Hanlon, A.R.M., Underwood, G.J.C., and Baker N.R. 2002, Marine Ecology-Progress Series, 228, 47.
224. Underwood, G.J.C., Perkins, R.G., Consalvey, M.C., Hanlon, A.R.M., Oxborough, K., Baker, N.R., and Paterson, D.M. 2005, Limnol. Oceanogr., 50, 755.
225. Velthuys, B. 1981, FEBS Lett., 126, 277.
226. Oxborough, K., and Baker, R. 1997, Plant Cell Environ., 20, 1473.
227. Balachandran, S., Osmond, C., and Daley, P. 1994, Plant Physiol., 104, 1059.
228. Ning, L., Edwards, G., Strobel, G., Daley, L., and Callis, J. 1995, Appl. Spectr., 49, 1381.
229. Ning, L., Petersen, B., Edwards, G., Daley, L., and Callis, J. 1997, Appl. Spectr., 51, 1.
230. Cardon, Z., Mott, K., and Berry, J. 1994, Plant Cell Environ., 17, 995.
231. Lichtenthaler, H.K., and Babani, F. 2000, Plant Physiol. Biochem., 38, 889.
232. Lichtenthaler, H.K., and Miehé, J. 1997, Trends Plant Sci., 2, 316.